Networks and Heterogeneous Media

http://www.aimspress.com/journal/nhm

NHM, 18(2): 694–722.
DOI: 10.3934/nhm.2023030
Received: 22 July 2022
Revised: 19 May 2022
Accepted: 11 January 2023
Published: 22 February 2023

Research article

Emissions minimization on road networks via Generic Second Order Models

Caterina Balzotti [1], **Maya Briani**[2,*] **and Benedetto Piccoli**[3]

[1] SISSA Scuola Internazionale Superiore di Studi Avanzati, Trieste, Italy
[2] Istituto per le Applicazioni del Calcolo, Consiglio Nazionale delle Ricerche, Rome, Italy
[3] Department of Mathematical Sciences, Rutgers University, Camden, USA

* **Correspondence:** Email: m.briani@iac.cnr.it.

Abstract: In this paper we consider the problem of estimating emissions due to vehicular traffic on complex networks, and minimizing their effect by regulating traffic at junctions. For the traffic evolution, we consider a Generic Second Order Model, which encompasses the majority of two-equations (i.e., second-order) models available in the literature, and extend it to road networks with merge and diverge junctions. The dynamics on the whole network is determined by selecting a solution to the Riemann Problems at junctions, i.e., the Cauchy problems with constant initial data on each incident road. The latter are solved by assuming the maximization of the flow and assigning a traffic distribution coefficient for outgoing roads of diverges, and a priority rule for incoming roads of merges. A general emission model is considered and its parameters are tuned to the NO_x emission rate. The minimization of emissions is then formulated in terms of the traffic distribution and priority parameters, taking into account travel times. A comparison is provided between roundabouts with optimized parameters and traffic lights, which correspond to time-varying traffic priorities. Our approach can be adapted to manage traffic in complex networks in order to reduce emissions while keeping travel time at acceptable levels.

Keywords: Second order traffic models; road networks; Riemann problem; emissions

1. Introduction

The aim of this paper is to build a model to estimate and minimize traffic emissions by regulating traffic dynamics. Such regulation corresponds to the choice of suitable model parameters, which in turn represent traffic signals and traffic light timing. Specifically, we extend the Generic Second Order Model (GSOM), introduced in [3,29], to road networks, pair it to an emission model and then minimize a functional comprising NO_x emissions and travel time.

Estimating traffic emissions is an important and challenging problem. First, most emission models

are based on the knowledge of vehicle speed and acceleration. Thus, at macroscopic level, a first-order system based only on conservation of cars, such as the Lighthill-Whitham-Richards (LWR) model [31,35], is not sufficient to feed an emission model. In particular, the LWR model admits solutions with unbounded acceleration [30] which would lead to unrealistic emissions estimates. It is then necessary to consider a so-called second-order model, i.e., a model with two equations: a first equation for the conservation of mass and a second for the conservation or balance of a modified momentum, which may model drivers' property. The first second-order model goes back to Payne and Whitham [33, 38]. After criticisms to the model, see [12], a new line of research originated starting with the Aw-Rascle-Zhang (ARZ) model [5, 39], which successfully addressed criticisms to the Payne-Whitham approach. More recently, various second-order models were proposed ranging from generalizations of the ARZ, such as in [14, 17], to phase transition models as in [8, 10] and GSOM in [3, 27, 29]. Such models are characterized by a family of fundamental diagrams (density-flow functions) and, due to their multi-faceted nature, are particularly appropriate to fit real traffic data. We refer to [15, 34] for more details on data-fitted second order models.

Traffic models on networks have been widely studied in last two decades and authors have considered many different traffic scenarios proposing a rich amount of alternative models at junctions. The LWR model has been extended to road networks in several papers, see for example [13, 18, 20, 25]. The ARZ model on networks was considered in [19, 23, 24] and phase-transition models in [11, 21]. In this paper we consider a road network with merge (two incoming and one outgoing roads) and diverge (one incoming and two outgoing roads) junctions. On each road, we assume that the traffic flow evolution is described by the GSOM

$$\begin{cases} \partial_t \rho + \partial_x(\rho v) = 0 \\ \partial_t w + v \partial_x w = 0, \end{cases} \tag{1.1}$$

where ρ is the density of vehicles, $v = V(\rho, w)$ is the velocity function, and w is a property of drivers. Notice that the first equation in (1.1) models the conservation of cars, while the second is the passive advection of the variable w, which gives rise to different fundamental diagrams. To define the solution on the whole network we follow the approach proposed in [18] based on the concept of Riemann Problem at a junction, which is a Cauchy problem with constant initial data on each road. Solutions to Riemann Problems are required to maximize the flux while conserving the density ρ and total property $y = \rho w$ through the junction. To determine a unique solution to Riemann Problems, we need to introduce additional criteria, which depend on the type of junction. For diverge junctions, a traffic distribution parameter is assigned to outgoing roads as done in [24] for the ARZ model. For merge junctions, a priority rule between incoming roads is considered, as it was done for the LWR model in [9]. More precisely, for a fixed priority parameter $\beta \in [0, 1]$, given the two incoming fluxes $\hat{q}_1$, $\hat{q}_2$, we require:

$$(1 - \beta)\, \hat{q}_2 = \beta\, \hat{q}_1. \tag{1.2}$$

Equation (1.2) establishes a proportional relationship between the two incoming fluxes. For instance, if $\beta = 0$ only traffic from the first road is allowed and vice versa for $\beta = 1$. Therefore, traffic lights can be easily represented by time-varying priority parameters. This rule, together with the maximization of flux and conservation of ρ and y, determines unique values of the variable w on each road. In fact, the value $\hat{w}_3$ on the outgoing road is given by a convex combination of the values $\hat{w}_1$ and $\hat{w}_2$ of the two

incoming roads, i.e.,

$$\hat{w}_3 = (1-\beta)\hat{w}_1 + \beta\hat{w}_2. \tag{1.3}$$

As a result, the maximal flux that can be received by the outgoing road, i.e. the supply, depends on the priority rule. The final solution is determined by maximizing the flow through the junction respecting the priority rule, but relaxing the latter in case the supply exceeds the demand from the road with higher priority. In rough words, the supply is given to incoming roads according to the priority rule and redistributed in case of surplus. The complete procedure to build the solution for a merge junction is explained in details in Definition 3.4. The extension of the proposed algorithms to a generic junction with n incoming and m outgoing roads can be found in [6] together with some preliminary results on the bounds on the total variation of junction waves.

The solution on networks to GSOM is then used to feed an emission model, focusing on the emission of nitrogen oxides (NO_x). Several studies deal with estimating emissions from dynamic traffic models, see for instance [1, 2, 7, 22, 26, 36, 37] and references therein. In particular, in [2] the authors deal with minimizing emissions by acting on the parameters of the model, while in [22] the authors analyze the possible benefits on emissions deriving from the limitation of traffic. The interest on NO_x gases in our work is due to their negative effects on health [40] and to their connection with ozone [4]. Minimizing only emissions would result in extreme solutions blocking traffic, thus we consider a cost function including a term measuring travel times. Therefore, we express the cost of emissions and travel time over the whole network as:

$$\mathcal{F}(\gamma) = \sum_r \left(c_1 \int\int E_r^\gamma(x,t)dxdt + c_2 \int\int \frac{1}{\mathcal{V}_r^\gamma(x,t)} dxdt \right),$$

where E_r^γ, respectively $\mathcal{V}_r^\gamma$, is the emission rate, respectively velocity, along the road r, while c_1 and c_2 are weights. The functional $\mathcal{F}$ depends on the parameter vector γ governing the traffic dynamic, which is comprised of the traffic distribution and priority parameters. Our interest is in minimizing $\mathcal{F}(\gamma)$ and compare different type of intersections, such as traffic lights and roundabouts. Note that, we consider a control γ which varies in a compact set and therefore the minimum exists. Due the the high nonlinearity of $\mathcal{F}(\gamma)$, explicit analytical solutions can not be found in general. Therefore, we resort to numerical optimization to compute the optimal vectors γ. First, we focus on a merge junction and compare a priority-based junction with one regulated by a traffic light. The latter corresponds to alternating the values $\beta = 0$ and $\beta = 1$ for the green and red phases. These cycles are parameterized by the green-phase duration t_g and the red-phase duration t_r. The numerical results show that it is possible to find an optimal β and an optimal couple (t_g, t_r), and that the two types of junctions perform similarly when minimizing emissions and travel time.

Next, we analyze how the solution to the minimization problem depends on the initial traffic state (ρ, w). Here we interpret w as drivers' preferred speed: low values of w correspond to slow drivers, and high values of w to fast drivers. For the priority-ruled junction, the minimum of the functional is achieved by giving high priority to the incoming road with higher density and fast drivers. Similarly, for the traffic light, the road with higher density must have a longer green-phase, except for high congestion when the opposite happens. In the latter situation, the sensitivity with respect to w is greater.

We then focus on a more complex situation of a roundabout with two incoming and two outgoing roads. The roundabout has four additional stretch of roads to connect incoming to outgoing roads and form a circle. As before we compare priority-based junctions with traffic lights, by choosing optimally

the priorities and the traffic light timing. Further, we compare the results obtained by the optimal traffic light timing with a periodic one showing that the former is convenient especially in reducing travel times. The numerical tests show that, when few vehicles enter the network, traffic lights produce lower emissions and travel times compared to the priority-based case. In congested situations, instead, the use of priorities produces higher levels of emissions but with shorter travel times w.r.t. traffic lights dynamics. It is worth to notice that traffic light timing can be easily adjusted in time, while changing priority-based rule would be more challenging. Overall, traffic lights outperform traffic signals in terms of emissions for roundabouts and perform better also taking into account travel times for low densities. Moreover, the optimal traffic light timing are more robust for variation of the functional weights. Interestingly, there is an increasing diffusion of roundabouts in Europe and US given the expected better performance in terms of output. This study shows that traffic signals should be added to roundabouts if one aims also at lowering emissions. This is a first example of how the model can be used to support decision makers for sustainable traffic management.

The paper is organized as follows. In Section 2 we define the GSOM and the Riemann problem at junctions. In Section 3 we describe the solution to the Riemann problem for diverge and merge junctions. In Section 4 a functional is formulated to estimate emission rate and travel time, while in Section 5 we provide details for the numerical approach. Sections 6 and 7 are devoted to the numerical tests for optimal controls and estimation of NO_x emissions. In Section 8 we draw our conclusions. Finally, in Appendix A we report some additional numerical tests for the roundabout.

2. The Riemann Problem for GSOM at a junction

In order to extend the GSOM model to networks, one has to analyze the Riemann problem at a junction, i.e., the Cauchy problem with constant initial data on each road incident to the junction.

Recall the GSOM model equations (1.1). The variable w parametrizes a family of fundamental diagrams $Q(\rho, w) = \rho V(\rho, w)$. The usual assumptions on Q and V are:

(H1) $Q(0, w) = 0$ and $Q(\rho^{\max}(w), w) = 0$ for each w, where $\rho^{\max}(w)$ is the maximum density of vehicles for $Q(\cdot, w)$.

(H2) $Q(\rho, w)$ is strictly concave with respect to ρ, i.e., $\frac{\partial^2 Q}{\partial \rho^2} < 0$.

(H3) $Q(\rho, w)$ is non-decreasing with respect to w, i.e., $Q_w \geq 0$.

(H4) $V(\rho, w) \geq 0$ for each ρ and w.

(H5) $V(\rho, w)$ is strictly decreasing with respect to ρ, i.e., $V_\rho < 0$ for each w.

(H6) $V(\rho, w)$ is non-decreasing with respect to w, i.e., $V_w \geq 0$.

From (H2) and (H3), for every w the curve $\rho \to Q(\cdot, w)$ has a unique point of maximum, denoted by $\sigma(w)$, and we set $Q^{\max}(w) = Q(\sigma(w), w)$. Moreover, when $\rho = 0$ there is not a unique maximum velocity. For every w we set $V^{\max}(w) = V(0, w)$.

The eigenvalues of Eq (1.1) are

$$\lambda_1(\rho, w) = V(\rho, w) + \rho V_\rho(\rho, w) \tag{2.1}$$

$$\lambda_2(\rho, w) = V(\rho, w). \tag{2.2}$$

The concavity of the flux implies $\lambda_1 \leq \lambda_2$ and $\lambda_1 = \lambda_2$ if and only if $\rho = 0$, thus for $\rho \neq 0$ the system is strictly hyperbolic. The eigenvectors associated with the eigenvalues are

$$\gamma_1(\rho, w) = (\rho, \rho w) \quad \text{and} \quad \gamma_2(\rho, w) = \left(-\frac{1}{\rho} V_w(\rho, w), V_\rho(\rho, w) - \frac{1}{\rho^2} V_w(\rho, w)\right).$$

The first eigenvalue is genuinely nonlinear, i.e., $\nabla\lambda_1 \cdot \gamma_1 \neq 0$, while the second one is linearly degenerate, i.e., $\nabla\lambda_2 \cdot \gamma_2 = 0$. Hence, the curves of the first family are 1-shocks or 1-rarefaction waves, while the curves of the second family are 2-contact discontinuities. Finally the Riemann invariants are

$$\begin{aligned} z_1(\rho, w) &= w \\ z_2(\rho, w) &= V(\rho, w). \end{aligned}$$

The first Riemann invariant z_1 is constant along 1-shock and 1-rarefaction waves, while the second Riemann invariant z_2 is constant along the 2-contact discontinuities.

By defining the *total property* $y = \rho w$, Eq (1.1) can be rewritten in conservative form as

$$\begin{cases} \partial_t \rho + \partial_x(\rho v) = 0 \\ \partial_t y + \partial_x(y v) = 0 \end{cases}$$

where $v = V\left(\rho, \frac{y}{\rho}\right)$.

We recall now the main definitions concerning traffic models on road networks and we refer to [13, 18, 20, 25] for further details. A road is modeled by an interval $I = (a, b) \subset \mathbb{R}$, with possibly $a = -\infty$ or $b = +\infty$. A junction J is a collection of roads $((I_1, \dots, I_n), (I_{n+1}, \dots, I_{n+m}))$ where $I_1, \dots, I_n$ are the incoming roads and $I_{n+1}, \dots, I_{n+m}$ are the outgoing ones. We define a network as a couple $(\mathcal{I}, \mathcal{J})$ where $\mathcal{I}$ is a finite collection of roads I_r, and $\mathcal{J}$ is a finite collection of junctions J.
On each road I_r, the traffic dynamic is described by a GSOM as

$$\begin{cases} \partial_t \rho_r + \partial_x(\rho_r v_r) = 0 \\ \partial_t y_r + \partial_x(y_r v_r) = 0 \end{cases} \tag{2.3}$$

with $v_r = V\left(\rho_r, \frac{y_r}{\rho_r}\right)$, for $x \in I_r$ and $t \geq 0$. The construction of a solution on the whole network is obtained via wave-front tracking starting from solutions to Riemann problems to Eq (2.3) at each junction. More precisely, given constant initial data on each road, we look for possible waves with negative speed for incoming roads and positive ones on outgoing roads. This is necessary to have conservation of mass through the junction, see [18]. In the literature this construction is usually called Riemann Solver, which is a map that assigns a solution to each constant initial data on the roads of the network, see [18, Definition 4.2.2] for further details. To isolate the admissible waves, we study the sign of the eigenvalues in Eq (2.1) and Eq (2.2). By the concavity of the flux function, the first eigenvalue $\lambda_1(\rho, w) = \rho + \rho V_\rho(\rho, w) = Q_\rho(\rho, w)$ satisfies $\lambda_1 \geq 0$ for $\rho \leq \sigma(w)$ and $\lambda_1 < 0$ for $\rho > \sigma(w)$. The second eigenvalue is given by $\lambda_2(\rho, w) = V(\rho, w)$, thus by (H4) the speed of the 2-contact discontinuity is always non-negative.

In order to describe the flux maximization, let us consider the *supply* and *demand* functions, see [17] for details and discussion. The supply function $s(\rho, w)$ is defined as

$$s(\rho, w) = \begin{cases} Q^{\max}(w) & \text{if } \rho \leq \sigma(w) \\ Q(\rho, w) & \text{if } \rho > \sigma(w) \end{cases}, \tag{2.4}$$

and the demand function $d(\rho, w)$ as

$$d(\rho, w) = \begin{cases} Q(\rho, w) & \text{if } \rho \le \sigma(w) \\ Q^{\max}(w) & \text{if } \rho > \sigma(w) \end{cases}. \tag{2.5}$$

2.1. Incoming roads

Let us consider an incoming road at a junction. Only waves with negative speed are admissible. Since $\lambda_2 \ge 0$, we can have only 1-shock or 1-rarefaction waves.

We fix a left state $U^- = (\rho^-, w^-)$ and look for the set of all admissible right states $\hat{U} = (\hat{\rho}, \hat{w})$ that can be connected to U^- with waves with negative speed. Along the 1-waves the variable w is conserved, therefore only the density ρ changes. This case is analogous to the definition of admissible solutions on incoming roads for first order traffic models, see for instance [18]. We refer to [24] where the ARZ model is treated in a similar way.

Proposition 1. *Let V be a velocity function that verifies properties* (H4)–(H6) *and let $U^- = (\rho^-, w^-)$ be a left state on an incoming road.*
If $\rho^- = 0$, then the only admissible right state is $\hat{U} = U^-$.
If $\rho^- \neq 0$, then the set of possible right states $\hat{U} = (\hat{\rho}, \hat{w})$ verifies $\hat{w} = w^-$ and:

1. *If $\rho^- \le \sigma(w^-)$, then $\hat{\rho} \in \mathcal{N}(U^-) = \{\rho^-\} \cup (\widetilde{\rho}^-(w^-), \rho^{\max}(w^-)]$, where $\widetilde{\rho}^-(w^-)$ is the density such that $Q(\widetilde{\rho}^-(w^-), w^-) = Q(\rho^-, w^-)$.*
2. *If $\rho^- > \sigma(w^-)$, then $\hat{\rho} \in \mathcal{N}(U^-) = [\sigma(w^-), \rho^{\max}(w^-)]$.*

Moreover, denoting by d the demand function defined in Eq (2.5)*, it holds*

$$Q(\hat{\rho}, \hat{w}) \le d(\rho^-, w^-). \tag{2.6}$$

Proof. First assume $\rho^- \neq 0$. If $\rho^- \le \sigma(w^-)$ (Figure 1 top-left) to have $\lambda_1 \le 0$ there are two possibilities: either $\hat{U} = U^-$, or moving above the density value $\widetilde{\rho}^-(w^-) > \sigma(w^-)$ by a jump with zero speed. Indeed, since $Q(\widetilde{\rho}^-(w^-), w^-) = Q(\rho^-, w^-)$, the Rankine-Hugoniot condition $s(\widetilde{U}^- - U^-) = Q(\widetilde{\rho}^-(w^-), w^-) - Q(\rho^-, w^-)$ implies that the speed of the discontinuity s is zero. In this case we can move with a 1-shock with negative speed towards any right state $\hat{U}$ with $\hat{w} = w^-$ and $\widetilde{\rho}^-(w^-) < \hat{\rho} \le \rho^{\max}(w^-)$. If $\rho^- = 0$ then $\widetilde{\rho}^-(w^-) = \rho^{\max}(w^-)$, therefore the solution is $\hat{U} = U^-$.

If $\rho^- > \sigma(w^-)$, every state $\hat{U}$ with $\hat{w} = w^-$ and $\hat{\rho} \in [\sigma(w^-), \rho^{\max}(w^-)]$ is connected to U^- with waves with negative speed (Figure 1 top-right). In particular, we have a 1-rarefaction wave if $\hat{\rho} \le \rho^-$ and a 1-shock if $\hat{\rho} > \rho^-$.

□

2.2. Outgoing roads

Let us consider an outgoing road at a junction. We are interested in the waves with positive speed, thus we can have a 1-shock or 1-rarefaction wave and a 2-contact discontinuity.

We fix a right state $U^+ = (\rho^+, w^+)$ and look for the set of all admissible left states $\hat{U} = (\hat{\rho}, \hat{w})$ that can be connected to U^+ with waves with positive speed. We emphasize that along the 1-waves the w is

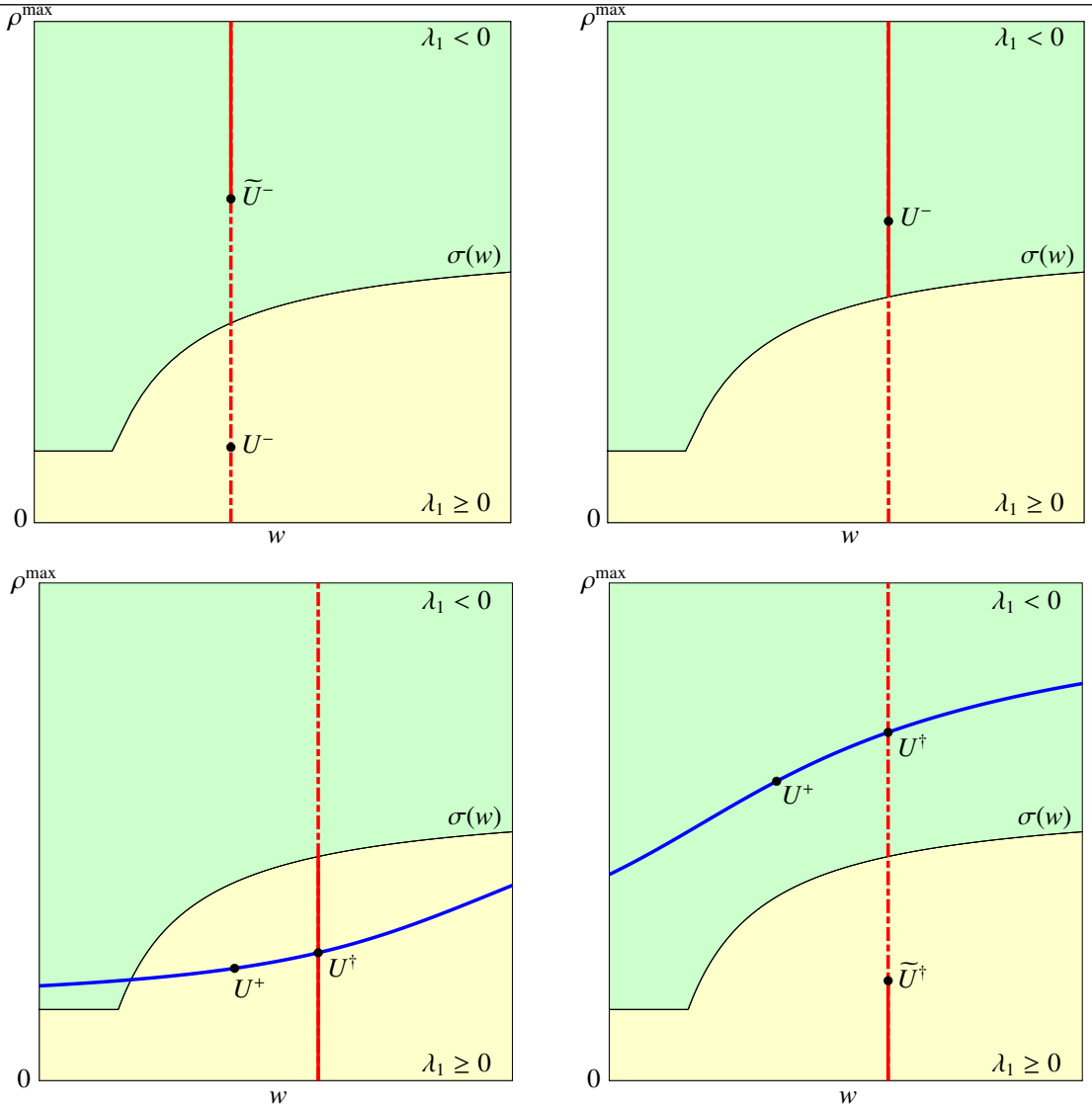

Figure 1. The function graphs refer to the CGARZ model [16] with the family of flux functions defined in Eqs (5.1)–(5.3). Top: two possible configurations of incoming road states. The red solid line identifies the set of all possible right states $\hat{U}$ reachable from the left state U^-. Bottom: two possible configurations of the state on an outgoing road. The red solid line identifies the set of possible left states $\hat{U}$ reachable from the right state U^+.

conserved and only the density ρ changes. We therefore assume that the value w^- is given and depends on the states on the incoming roads (see Section 3). On the other hand, along the 2-wave the velocity $V(\rho, w)$ is conserved. Then, the definition of the admissible states $\hat{U}$ depends on the existence of an intermediate point $U^\dagger = (\rho^\dagger, w^\dagger)$ such that $w^\dagger = w^-$ and $V(\rho^\dagger, w^\dagger) = V(\rho^+, w^+)$.

Proposition 2. *Let V be a velocity function that verifies properties* (H4)–(H6). *For a given value w^- and a given right state $U^+ = (\rho^+, w^+)$ with associated velocity $v^+ = V(\rho^+, w^+)$, if $v^+ \leq V^{\max}(w^-)$ then there exists a unique point $U^\dagger = (\rho^\dagger, w^\dagger)$ such that $w^\dagger = w^-$ and $V(\rho^\dagger, w^\dagger) = v^+$.*

Proof. If $v^+ \leq V^{\max}(w^-)$ then the equation $V(\rho, w^-) = v^+$ admits a solution. By (H5), $\partial_\rho V < 0$ and, by

the implicit function theorem, there exists $\rho(w; v^+)$ such that $V(\rho(w; v^+), w) = v^+$. Moreover, (H5)–(H6) imply

$$\frac{d\rho}{dw}(w; v^+) = -\partial_w V / \partial_\rho V \geq 0.$$

We then have $w^\dagger = w^-$ and $\rho^\dagger = \rho(w^-; v^+)$. □

Proposition 3. *Let V be a velocity function that verifies properties* (H4)–(H6)*, $U^+ = (\rho^+, w^+)$ a right state on an outgoing road, and $v^+ = V(\rho^+, w^+)$ the associated velocity. For a given value w^-, a left state $\hat{U} = (\hat{\rho}, \hat{w})$, which can be connected to U^+ with positive speed waves, satisfies $\hat{w} = w^-$ and the following.*

(i) If $v^+ \leq V^{\max}(w^-)$, let $U^\dagger = (\rho^\dagger, w^\dagger)$ be the intersection point between the level curves $\{z_2 = v^+\}$ and $\{z_1 = w^-\}$, then $w^\dagger = w^-$ and

1. *if $\rho^\dagger \leq \sigma(w^\dagger)$, then $\hat{\rho} \in \mathcal{P}(U^+) = [0, \sigma(w^\dagger)]$;*
2. *if $\rho^\dagger > \sigma(w^\dagger)$, then $\hat{\rho} \in \mathcal{P}(U^+) = [0, \widetilde{\rho}^\dagger(w^\dagger)) \cup \{\rho^\dagger\}$, where $\widetilde{\rho}^\dagger(w^\dagger)$ is the density such that $Q(\widetilde{\rho}^\dagger(w^\dagger), w^\dagger) = Q(\rho^\dagger, w^\dagger)$.*

(ii) If $v^+ > V^{\max}(w^-)$ then $\hat{\rho} \in \mathcal{P}(U^+) = [0, \sigma(w^-)]$.

Moreover, denoting by s the supply function defined in Eq (2.4)*, it holds*

$$Q(\hat{\rho}, \hat{w}) \leq s(\rho^\dagger, w^\dagger). \tag{2.7}$$

Proof. If $v^+ \leq V^{\max}(w^-)$, by Proposition 2 there exists a unique point $U^\dagger$ such that $w^\dagger = w^-$ and $V(\rho, w^\dagger) = v^+$. Thus, if $\rho^\dagger \leq \sigma(w^\dagger)$, then every state $\hat{U}$ with $\hat{w} = w^-$ and $\hat{\rho} \in [0, \sigma(w^\dagger)]$ can be connected to $U^\dagger$ by waves with positive speed (Figure 1 bottom-left). In particular we have a 1-rarefaction wave if $\rho^\dagger \leq \hat{\rho}$ and a 1-shock if $\rho^\dagger > \hat{\rho}$. Then, $U^\dagger$ is connected to U^+ by a 2-contact discontinuity which has positive speed.

If $\rho^\dagger > \sigma(w^\dagger)$ (Figure 1 bottom-right), we have two possibilities: no wave, then $\hat{U} = U^\dagger$, or moving below the density value $\widetilde{\rho}^\dagger(w^\dagger) < \sigma(w^\dagger)$ by a jump with positive speed. In this case, a 1-rarefaction connects to an intermediate state $\hat{U}$ with $\hat{w} = w^\dagger$ and $0 \leq \hat{\rho} \leq \widetilde{\rho}^\dagger(w^\dagger)$, then a 2-contact discontinuity connects to U^+.

Otherwise, if $v^+ > V^{\max}(w^-)$ then the equality $V(\rho, w^-) = v^+$ can not hold. It holds $\rho^\dagger = 0$ and the admissible left state $\hat{\rho}$ has to be in $[0, \sigma(w^-)]$. □

To summarize, we denote

$$\rho^\dagger(w^-; v^+) = \begin{cases} \rho(w^-; v^+) & \text{if } v^+ \leq V^{\max}(w^-) \\ 0 & \text{if } v^+ > V^{\max}(w^-) \end{cases} \tag{2.8}$$

where $\rho(\cdot; v^+)$ is the implicit function given by the equation $V(\rho, w) = v^+$, which is well defined as stated in Proposition 2.

Remark 1. For numerical purposes, we use the Collapsed Generalized Aw-Rascle-Zhang (CGARZ) model, see [16] and Section 5. This model is characterized by a maximum velocity $V^{\max}$ common to any w. Hence, the case of $v^+ > V^{\max}(w)$ never holds for the CGARZ model.

3. The GSOM on networks

In this section we apply Propositions 1 and 3 to define the Riemann Solver for merge and diverge junctions. To identify a unique solution we assume the maximization of the flux and the conservation of ρ and $y = \rho w$ across the junction. Moreover, we assume that a distribution parameter on outgoing roads and a priority rule on incoming ones are given.

3.1. Diverge junction

We consider the case of a junction with one incoming and two outgoing roads. Given a left state U_1^- for the incoming road and two right states U_2^+ and U_3^+ for the outgoing roads, our aim is to determine the junction values $\hat{U}_i = (\hat{\rho}_i, \hat{w}_i)$, $i = 1, 2, 3$, giving rise to a boundary-value problem on each road. The solutions to the latter pieced together provide a solution to the Riemann problem at the junction.
First, introduce a traffic distribution parameter $\alpha \in (0, 1)$: vehicles are distributed in proportion α and $1 - \alpha$ on the roads 2 and 3, respectively. Note that the cases $\alpha = 0$ or $\alpha = 1$ reduce the problem to a simple 1 to 1 junction, thus in this analysis we exclude the two extreme values.
Set $\hat{q}_i = \hat{\rho}_i \hat{v}_i$, $\hat{v}_i = V(\hat{\rho}_i, \hat{w}_i)$, $i = 1, 2, 3$, then the conservation of ρ and y across the junction reads:

$$\alpha \hat{q}_1 = \hat{q}_2 \tag{3.1}$$

$$\alpha \hat{q}_1 \hat{w}_1 = \hat{q}_2 \hat{w}_2 \tag{3.2}$$

$$(1 - \alpha)\hat{q}_1 = \hat{q}_3 \tag{3.3}$$

$$(1 - \alpha)\hat{q}_1 \hat{w}_1 = \hat{q}_3 \hat{w}_3. \tag{3.4}$$

By Proposition 1 we have $\hat{w}_1 = w_1^-$, and by Eqs (3.1)–(3.4) we deduce $\hat{w}_1 = \hat{w}_2$ and $\hat{w}_1 = \hat{w}_3$, hence $\hat{w}_2 = \hat{w}_3 = w_1^-$. Now the states $\hat{U}_i$ correspond to six unknowns for which we have five equations. Using the free parameter $q = \hat{q}_1$ and, by Eqs (2.6) and (2.7) we get the constraints

$$\begin{aligned} &0 \le q \le d(\rho_1^-, w_1^-) \\ &0 \le \alpha q \le s(\rho_2^\dagger, w_1^-) \\ &0 \le (1 - \alpha) q \le s(\rho_3^\dagger, w_1^-), \end{aligned} \tag{3.5}$$

where, by Proposition 3, $w_2^\dagger = w_3^\dagger = w_1^-$ and $\rho_2^\dagger$, $\rho_3^\dagger$ are given by Eq (2.8) with $w^- = w_i^-$ and $v^+ = v_i^+$, $i = 2, 3$, respectively. To satisfy Eq (3.5) and maximize the outgoing flux, it holds

$$q = \min\{d(\rho_1^-, w_1^-), s(\rho_2^\dagger, w_1^-)/\alpha, s(\rho_3^\dagger, w_1^-)/(1 - \alpha)\}$$

and

$$\hat{q}_1 = q, \quad \hat{q}_2 = \alpha q, \quad \hat{q}_3 = (1 - \alpha) q.$$

Then, the junction density values are $\hat{\rho}_1 \in \mathcal{N}(U_1^-)$ such that $Q(\hat{\rho}_1, w_1^-) = \hat{q}_1$ and $\hat{\rho}_j \in \mathcal{P}(U_j^+)$ such that $Q(\hat{\rho}_j, w_j^-) = \hat{q}_j$, $j = 2, 3$. In [24, 28], the authors obtain the same solution for the ARZ model.

3.2. Merge junction

We consider the case of a junction with two incoming and one outgoing roads. Given two states U_1^- and U_2^- for the incoming roads and a state U_3^+ for the outgoing road, we look for the junction values

$\hat{U}_1$, $\hat{U}_2$ and $\hat{U}_3$. As done before, we set $\hat{q}_i = \hat{\rho}_i \hat{v}_i$, $i = 1, 2, 3$, and we assume that vehicles from roads 1 and 2 enter into the road 3 with the following priority rule

$$(1-\beta)\hat{q}_2 = \beta \hat{q}_1, \tag{3.6}$$

where $\beta \in [0, 1]$. Note that for $\beta = 0$ or $\beta = 1$, one of the two incoming roads is completely stopped at the junction, and the problem reduces to the 1 to 1 case.
The conservation of ρ and y across the junction yields:

$$\hat{q}_1 + \hat{q}_2 = \hat{q}_3 \tag{3.7}$$

$$\hat{q}_1 \hat{w}_1 + \hat{q}_2 \hat{w}_2 = \hat{q}_3 \hat{w}_3. \tag{3.8}$$

By Proposition 1, we have that $\hat{w}_1 = w_1^-$ and $\hat{w}_2 = w_2^-$. Equation (3.7) combined with Eqs (3.6) and (3.8), implies

$$\hat{w}_3 = (1-\beta) w_1^- + \beta w_2^-. \tag{3.9}$$

Hence, $\hat{w}_1$, $\hat{w}_2$ and $\hat{w}_3$ are defined and $\hat{q}_1$, $\hat{q}_2$ and $\hat{q}_3$ have to satisfy Eqs (3.6) and (3.7). It remains a free parameter and, in order to define a unique solution, we impose the maximization of the flux on the outgoing road. By Eqs (2.6) and (2.7), we get the constraints

$$\begin{aligned} 0 \le \hat{q}_1 &\le d(\rho_1^-, w_1^-) \\ 0 \le \hat{q}_2 &\le d(\rho_2^-, w_2^-) \\ 0 \le \hat{q}_3 &\le s(\rho_3^\dagger, \hat{w}_3), \end{aligned} \tag{3.10}$$

where $\rho_3^\dagger$ is given by Eq (2.8) with $w^- = \hat{w}_3$ and $v^+ = V(\rho_3^+, w_3^+)$. From now on, we set

$$d_1 = d(\rho_1^-, w_1^-) \text{ and } d_2 = d(\rho_2^-, w_2^-).$$

We assume that both d_1 and d_2 are greater than 0. Indeed, the trivial case of $d_1 = d_2 = 0$ means that no vehicles cross the intersection, and the case of $d_1 = 0$ or $d_2 = 0$ reduces the junction to the 1 to 1 type. In order maximize the flux on the outgoing road we set in Eq (3.10)

$$\hat{q}_3 = s(\rho_3^\dagger, \hat{w}_3). \tag{3.11}$$

To summarize, the couple $(\hat{q}_1, \hat{q}_2)$ is given by the intersection point P between the following two lines

$$\mathrm{r} : q_2 = \frac{\beta}{1-\beta} q_1 \tag{3.12}$$

$$\mathrm{s} : q_2 = s(\rho_3^\dagger, \hat{w}_3) - q_1, \tag{3.13}$$

where the first one represents the priority rule Eq (3.6), while the second one represent the conservation equation (3.7) coupled with Eq (3.11). In Eq (3.12), r coincides with the axis $x = 0$ when $\beta = 1$. Note that, since $\rho_3^\dagger = \rho_3^\dagger(\hat{w}_3; v_3^+)$ and $\hat{w}_3$ depends on β, the maximum flux that can be received by the outgoing road is a function of the priority rule, i.e., $s(\rho_3^\dagger, \hat{w}_3) = s_3(\beta)$.
The intersection point between r and s is

$$P = ((1-\beta)s_3(\beta), \beta s_3(\beta)). \tag{3.14}$$

If $P \in \Omega = [0, d_1] \times [0, d_2]$, we can set $\hat{q}_1 = (1-\beta)s_3(\beta)$ and $\hat{q}_2 = \beta s_3(\beta)$. Otherwise, if $P \notin \Omega$, then the point does not satisfy the constraints (3.10), and we need to *relax* one of our constraints. We propose two possible approaches:

(RP) The relation Eq (3.6) is satisfied with β fixed a priori, while the outgoing flow in Eq (3.11) is not maximized. This is the case for instance of a stop sign or a traffic policeman regulating the junction.

(AP) The priority parameter β is modified, thus allowing to maximize the outgoing flux. This is the case, for instance, of unsupervised junction.

To detail the procedure to compute the junction densities $\hat{\rho}_i$, $i = 1, 2, 3$, first recall that $\hat{w}_1 = \hat{w}_2 = w_1^-$ and $\hat{w}_3 = (1-\beta)w_1^- + \beta w_2^-$ as stated in Eq (3.9). We introduce the parameter

$$\beta_d = \frac{d_2}{d_1 + d_2} \tag{3.15}$$

which identifies the priority line in Eq (3.12) that passes through the point (d_1, d_2). If $P \notin \Omega$, we distinguish two cases:

(i) $\beta \geq \beta_d$ then the y-coordinate of P, $\beta s_3(\beta)$ is greater than the upper bound d_2. Then we fix $\hat{q}_2 = d_2$ and look for an admissible value $\hat{q}_1$;

(ii) $\beta < \beta_d$ then the x-coordinate $(1-\beta)s_3(\beta) > d_1$. Then we fix $\hat{q}_1 = d_1$ and look for an admissible value $\hat{q}_2$.

We first describe the RP algorithm. For a given priority parameter $\bar{\beta} \in [0, 1]$, to satisfy the priority rule, the solution must lie on the line $(1-\bar{\beta})\hat{q}_2 = \bar{\beta}\hat{q}_1$. For this reason, when $P \notin \Omega$ the couple $(\hat{q}_1, \hat{q}_2)$ will be defined by the intersection point between the priority line and the boundary $\partial\Omega$, see for instance the point Q in Figures 2b and 2c.

Definition 3.1. Riemann Solver Algorithm RP. Let $\bar{\beta} \in [0, 1]$ and let $\hat{w}_3$ and P be as in Eq (3.9) and Eq (3.14) with $\beta = \bar{\beta}$, respectively. Assume that Eq (3.7) holds. Define $(\hat{q}_1, \hat{q}_2) \in \Omega$ as follows:

1. If $P \in \Omega$, then $\hat{q}_1 = (1-\bar{\beta})s_3(\bar{\beta})$ and $\hat{q}_2 = \bar{\beta}s_3(\bar{\beta})$.
2. If $P \notin \Omega$ and $\bar{\beta} \geq \beta_d$, then $\hat{q}_1 = (1-\bar{\beta})d_2/\bar{\beta}$ and $\hat{q}_2 = d_2$.
3. If $P \notin \Omega$ and $\bar{\beta} < \beta_d$, then $\hat{q}_1 = d_1$ and $\hat{q}_2 = \bar{\beta}d_1/(1-\bar{\beta})$.

The density value $\hat{\rho}_i \in \mathcal{N}(U_i^-)$ is determined by the equality $Q(\hat{\rho}_i, \hat{w}_i) = \hat{q}_i$, $i = 1, 2$, while $\hat{\rho}_3 \in \mathcal{P}(U_3^+)$ is determined by $Q(\hat{\rho}_3, \hat{w}_3) = \hat{q}_3$.

To describe the AP algorithm we need some preliminary results.

Lemma 3.2. *The supply function $s(\rho_3^\dagger(w;\cdot), w)$ is non-decreasing in w.*

Proof. By Eq (2.4) we can have

$$s(\rho_3^\dagger(w;\cdot), w) = Q^{\max}(w) \quad \text{or} \quad s(\rho_3^\dagger(w;\cdot), w) = \rho_3^\dagger(w;\cdot)V(\rho_3^\dagger(w;\cdot), w).$$

In the first case, assumption (H3) applies; in the second one, by Proposition 2 we have $V(\rho_3^\dagger(w;\cdot), w) = v_3^+$ and $\rho_3^\dagger(w;\cdot)$ is non-decreasing in w. □

To study the function $s_3(\beta) = s(\rho_3^\dagger(\hat{w}_3(\beta);\cdot), \hat{w}_3(\beta))$ with respect to β, we distinguish two cases:

(a) $w_1^- \leq w_2^-$ then both $\hat{w}_3$ and s_3 are increasing in β;

(b) $w_1^- > w_2^-$ then both $\hat{w}_3$ and s_3 are decreasing in β.

Lemma 3.3. *Let $\bar{\beta} \in [0,1]$ and β_d given in Eq* (3.15).

1. *If $\bar{\beta} \geq \beta_d$ and $\bar{\beta} s_3(\bar{\beta}) > d_2$, then there exists at least a $\beta \in [0, \bar{\beta})$ such that $\beta s_3(\beta) = d_2$.*
2. *If $\bar{\beta} < \beta_d$ and $(1-\bar{\beta}) s_3(\bar{\beta}) > d_1$, then there exists at least a $\beta \in (\bar{\beta}, 1]$ such that $(1-\beta) s_3(\beta) = d_1$.*

Proof. We first prove point 1. Consider the two cases (a) and (b), i.e. $w_1^- < w_2^-$ and $w_1^- > w_2^-$, respectively.
If $w_1^- < w_2^-$ then the function $f(\beta) = \beta s_3(\beta)$ is increasing in $[0,1]$ and such that $f(0) = 0$ and $f(\bar{\beta}) > d_2$ by hypothesis; therefore, there exists a unique $\beta^* < \bar{\beta}$ such that $f(\beta^*) = d_2$.
If $w_1^- > w_2^-$ then $s_3(\beta)$ is decreasing in β and the behavior of the function $f(\beta) = \beta s_3(\beta)$ is not known a priori. However the function f is continuous and such that $f(0) = 0$ and $f(\bar{\beta}) > d_2$ by hypothesis; therefore there exists at least a $\beta < \bar{\beta}$ such that $f(\beta) = d_2$.
The proof of point 2 is entirely similar, so we skip the details. □

The AP algorithm is described in the following definition. As mentioned above, the algorithm adapts the priority parameter to maximize the outgoing flux while keeping the parameter as close as possible to its initial value.

Definition 3.4. Riemann Solver Algorithm AP. Let $\bar{\beta} \in [0,1]$ and P be as in Eq (3.14) with $\beta = \bar{\beta}$. Assume that Eq (3.7) holds. Define $(\hat{q}_1, \hat{q}_2) \in \Omega$ as follows:

1. If $P \in \Omega$ then $\hat{q}_1 = (1-\bar{\beta}) s_3(\bar{\beta})$, $\hat{q}_2 = \bar{\beta} s_3(\bar{\beta})$ and $\hat{w}_3 = (1-\hat{\beta}) w_1^- + \hat{\beta} w_2^-$ with $\hat{\beta} = \bar{\beta}$.
2. If $P \notin \Omega$ and $\bar{\beta} \geq \beta_d$, then for $\beta^* = \max\{\beta \in [0, \bar{\beta}) : \beta s_3(\beta) = d_2\}$, we set $\hat{\beta} = \max\{\beta^*, \beta_d\}$, $\hat{q}_1 = \min\{(1-\hat{\beta}) s_3(\hat{\beta}), d_1\}$, $\hat{q}_2 = d_2$ and $\hat{w}_3 = (1-\hat{\beta}) w_1^- + \hat{\beta} w_2^-$.
3. If $P \notin \Omega$ and $\bar{\beta} < \beta_d$, then for $\beta^* = \min\{\beta \in (\bar{\beta}, 1] : (1-\beta) s_3(\beta) = d_1\}$, we set $\hat{\beta} = \min\{\beta^*, \beta_d\}$, $\hat{q}_1 = d_1$, $\hat{q}_2 = \min\{\hat{\beta} s_3(\hat{\beta}), d_2\}$ and $\hat{w}_3 = (1-\hat{\beta}) w_1^- + \hat{\beta} w_2^-$.

The density value $\hat{\rho}_i \in \mathcal{N}(U_i^-)$ is determined by the equality $Q(\hat{\rho}_i, \hat{w}_i) = \hat{q}_i$, $i = 1, 2$, while $\hat{\rho}_3 \in \mathcal{P}(U_3^+)$ is determined by $Q(\hat{\rho}_3, \hat{w}_3) = \hat{q}_3$.

Proposition 4. *The couple $(\hat{q}_1, \hat{q}_2)$ in Definition 3.4 satisfies the constraints in Eq* (3.10).

Proof. The given couple $(\hat{q}_1, \hat{q}_2)$ verifies the first two constraints in Eq (3.10) by construction. Therefore, it remains to prove that $\hat{q}_3 = \hat{q}_1 + \hat{q}_2 \leq s_3(\hat{\beta}) = s_3(\rho_3^\dagger(\hat{w}_3; \cdot), \hat{w}_3)$.

We start from the case 2 of Definition 3.4. In light of Lemma 3.3 case 1, the value β^* is well defined. Moreover, since the slope of r increases with β, the point $((1-\beta^*) s_3(\beta^*), d_2)$ is such that: if $\beta^* \geq \beta_d$ then $(1-\beta^*) s_3(\beta^*) \leq d_1$ and if $\beta^* > \beta_d$ then $(1-\beta^*) s_3(\beta^*) > d_1$. Therefore, we focus on these two possibilities:

- If $\beta^* \geq \beta_d$ then $\hat{\beta} = \beta^*$ and $\hat{q}_1 = (1-\hat{\beta}) s_3(\hat{\beta})$. Hence, $\hat{q}_1 + \hat{q}_2 = (1-\hat{\beta}) s_3(\hat{\beta}) + d_2 = (1-\hat{\beta}) s_3(\hat{\beta}) + \hat{\beta} s_3(\hat{\beta}) = s_3(\hat{\beta})$ and the thesis follows. This is the case, for instance, of point R in Figure 2b.

- If $\beta^* < \beta_d$ then $\hat{\beta} = \beta_d$ and $\hat{q}_1 = d_1$. The couple $(\hat{q}_1, \hat{q}_2) = (d_1, d_2)$ is admissible if $d_1 + d_2 \le s_3(\beta_d)$. Since $d_1 = (1 - \beta_d)d_2/\beta_d$ we have $d_1 + d_2 = d_2/\beta_d$. From the definition of β^*, for each $\beta \in (\beta^*, \bar{\beta}]$ it holds $\beta s_3(\beta) > d_2$, and we get the thesis:

$$d_1 + d_2 = \frac{d_2}{\beta_d} < \frac{\beta_d s_3(\beta_d)}{\beta_d} = s_3(\beta_d).$$

  This is the case of point S in Figure 2b.

The proof of case 3 follows similarly, see Figure 2c for an example of possible configuration. □

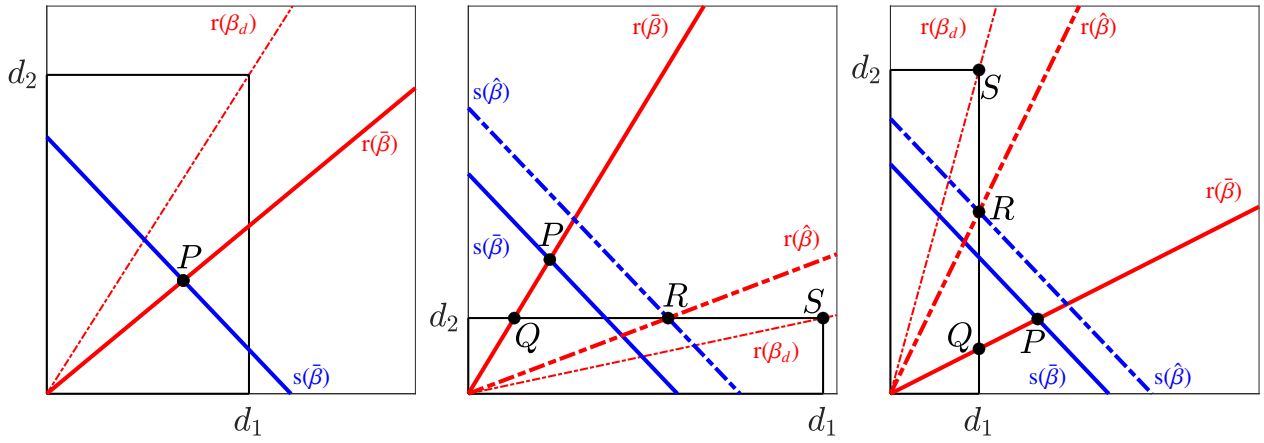

(a) $P \in \Omega$. **(b)** $P \notin \Omega$ and $\bar{\beta} \ge \beta_d$ **(c)** $P \notin \Omega$ and $\bar{\beta} < \beta_d$.

Figure 2. The three possible cases defining the RP and AP algorithms, with P in Eq (3.14), β_d in Eq (3.15), $\bar{\beta} \in [0, 1]$ and $\hat{\beta}$ in Definition 3.4. The red and blue lines represent r and s defined in Eq (3.12) and Eq (3.13), respectively, for different values of β. For both algorithms, plot (a) represents case 1, plot (b) shows case 2 with $w_1^- > w_2^-$ and plot (c) shows case 3 with $w_1^- < w_2^-$.

Remark 2. Let us consider the particular case of $w_1^- = w_2^- = w_3^+$, i.e., the variable w is constant on the roads network. The diverge junction can be treated exactly as the LWR model at junctions, as done in [18]. For the merge junction we observe that the assumption of w constant implies that the straight line s defined in Eq (3.13) coincides for all β, therefore the solution is limited to the points P or Q in Figure 2, excluding the points R and S. Thus, we recover again the LWR model on networks, as treated in [18].

4. Minimize emissions and travel time

The emission of pollutants is strictly connected to speed and acceleration of vehicles. In this section we set up an optimization problem to minimize the NO_x emission rates due to vehicular traffic.

Consider Eq (2.3) on a network with roads I_r, $r = 1, \dots, N_r$, during a time interval $[0, T]$. Following [7], we use the microscopic emission model proposed in [32] which estimates the emission rate E_i of vehicle i at time t using the instantaneous speed $v_i(t)$ and acceleration $a_i(t)$. We then define

$$E_i(t) = \max\{E_0, f_1 + f_2 v_i(t) + f_3 v_i(t)^2 + f_4 a_i(t) + f_5 a_i(t)^2 + f_6 v_i(t) a_i(t)\}. \tag{4.1}$$

where E_0 is a lower-bound of emission and f_1 to f_6 are emission constants associated with NO_x, see Table 1.

Table 1. NO_x parameters in emission model (4.1).

Vehicle mode	$f_1\left[\frac{g}{s}\right]$	$f_2\left[\frac{g}{m}\right]$	$f_3\left[\frac{g\,s}{m^2}\right]$	$f_4\left[\frac{g\,s}{m}\right]$	$f_5\left[\frac{g\,s^3}{m^2}\right]$	$f_6\left[\frac{g\,s^2}{m^2}\right]$
If $a_i(t) \geq -0.5\,m/s^2$	6.19e-04	8e-05	–4.03e-06	–4.13e-04	3.80e-04	1.77e-04
If $a_i(t) < -0.5\,m/s^2$	2.17e-04	0	0	0	0	0

Let $\Gamma \subset \mathbb{R}^k$ be the set of k control parameters $\gamma = (\gamma_1, \ldots, \gamma_k)$ governing the traffic dynamic. These are given by the traffic distribution and priority parameters α and β of Section 3. Let N_r be the number of roads and $E_r^\gamma(x,t)$ be the emission rate in x at time t related to γ and road r. Note that $E_r^\gamma(x,t)$ is estimated through Eq (4.1) by summing all the vehicle contributions in x at time t. We introduce the following operator to estimate the total emission rate on a road network as a function of $\gamma \in \Gamma$,

$$\mathcal{F}_E(\gamma) = \sum_{r=1}^{N_r} \int_0^T \int_0^L E_r^\gamma(x,t)dxdt. \tag{4.2}$$

To guarantee acceptable travel times, we include a velocity term thus getting the objective function

$$\mathcal{F}(\gamma) = \sum_{r=1}^{N_r} \left(c_1 \int_0^T \int_0^L E_r^\gamma(x,t)dxdt + c_2 \int_0^T \int_0^L \frac{1}{\mathcal{V}_r^\gamma(x,t)}dxdt \right), \tag{4.3}$$

where c_1 and c_2 are two proper weights and $\mathcal{V}_r^\gamma = \max\{V_r^\gamma(x,t), \varepsilon\}$, $\varepsilon > 0$, with V_r^γ velocity function of the traffic model, related to control parameter γ and to road r. The parameter ε allows to exclude the null speeds in the calculation. Our goal is to solve the minimization problem

$$\min_{\gamma \in \Gamma} \mathcal{F}(\gamma). \tag{4.4}$$

The minimum exists since Γ is a compact set in $\mathbb{R}^k$, but we do not expect uniqueness. Due to the complexity and the strictly nonlinear dependence of the functional $\mathcal{F}$ on the control γ, we treat the problem numerically using global search.

5. Numerical setup

From the GSOM family, we choose the CGARZ model [16] for simulations. The CGARZ model assumes that there is a unique maximum density $\rho^{\max}$ independent of w at which the vehicles stop, i.e. $V(\rho^{\max}, w) = 0$ for all w. Furthermore, it assumes a given *free-flow threshold density* ρ_f such that the flux of vehicles is not influenced by w when $\rho \leq \rho_f$ (*free-flow regime*). Thus, the flux is described by a single-valued fundamental diagram in free-flow regimes and by a multi-valued function in congestion. For $\rho \in [0, \rho^{\max}]$, we have

$$Q(\rho, w) = \begin{cases} Q_f(\rho) & \text{if } 0 \leq \rho \leq \rho_f \\ Q_c(\rho, w) & \text{if } \rho_f < \rho \leq \rho^{\max}. \end{cases} \tag{5.1}$$

Following [7], we assume a lower and upper bound for w, i.e., $0 \le w_L \le w \le w_R$, a Greenshields flux function in the free-flow phase, i.e.,

$$Q_f(\rho) = \frac{V^{\max}}{\rho^{\max}} \rho \, (\rho^{\max} - \rho) \,, \tag{5.2}$$

and a flux in congested phase given by

$$Q_c(\rho, w) = \frac{V^{\max}}{\rho^{\max}} \, (\rho^{\max} - \rho) \, ((1 - \theta(w))\rho_f + \theta(w)\rho), \quad \theta(w) = \frac{w - w_L}{w_R - w_L}, \tag{5.3}$$

where $w_L = Q_f(\rho_f)$, $w_R = Q_f(\rho^{\max}/2)$ and $\rho^{\max}/2$ is the critical density of $Q_f(\cdot)$. The velocity function is then given by

$$V(\rho, w) = \frac{Q(\rho, w)}{\rho}.$$

With these choices, the property w describes drivers attitude with respect to speed. Low values of w describe *slow drivers*, and high values of w *fast drivers*.

We consider now the traffic model in Eq (2.3) with flux function given in Eq (5.1), and we divide each road into N_x cells $[x_{j-1/2}, x_{j+1/2})$ of length Δx centered in x_j, and the time interval into $N_t + 1$ steps $t^n = n\Delta t$.

The model is then solved numerically with the 2CTM scheme [7] with suitable boundary conditions at the extremes of the network. We use the theory given in Sections 3.1 and 3.2 to build the numerical solution at junctions.

The 2CTM numerical scheme is described by the two equations

$$\begin{aligned} \rho_{r,j}^{n+1} &= \rho_{r,j}^{n} - \frac{\Delta t}{\Delta x}(F_{r,j+1/2}^{\rho,n} - F_{r,j-1/2}^{\rho,n}) \\ y_{r,j}^{n+1} &= y_{r,j}^{n} - \frac{\Delta t}{\Delta x}(F_{r,j+1/2}^{y,n} - F_{r,j-1/2}^{y,n}), \end{aligned}$$

where $F_{r,j\pm1/2}^{\rho,n}$ and $F_{r,j\pm1/2}^{y,n}$ are the numerical fluxes, ρ_j^n and y_j^n are the j-cell average

$$\rho_j^n = \frac{1}{\Delta x} \int_{x_{j-1/2}}^{x_{j+1/2}} \rho(x, t^n) dx, \quad y_j^n = \frac{1}{\Delta x} \int_{x_{j-1/2}}^{x_{j+1/2}} y(x, t^n) dx,$$

for any time t^n, respectively. For the CGARZ model, the numerical fluxes are defined as

$$F_{r,j-1/2}^{\rho,n} = \min\{d(\rho_{r,j-1}^n, w_{r,j-1}^n), s(\rho_{r,j}^n, w_{r,j}^n)\} \tag{5.4}$$

where $d(\cdot,\cdot)$ and $s(\cdot,\cdot)$ are the demand and supply functions defined in Eqs (2.5) and (2.4) respectively. Since $y = \rho w$ the numerical fluxes $F_{r,j\pm1/2}^{y,n}$ are such that

$$F_{r,j-1/2}^{y,n} = w_{r,j-1}^n F_{r,j-1/2}^{\rho,n} \qquad \text{and} \qquad F_{r,j+1/2}^{y,n} = w_{r,j}^n F_{r,j+1/2}^{\rho,n}.$$

Moreover, the stability of the scheme is guaranteed by the CFL condition

$$\Delta t \le \Delta x / (2V^{\max}), \tag{5.5}$$

where for the CGARZ model $V^{\max} = V(0, w)$ for all w. See [7] and references therein for more details.

The emission model (4.1) is based on vehicles speed and acceleration. The latter is obtained by computing the total derivative of $V(\rho, w)$, i.e.,

$$a(x,t) = \frac{Dv(x,t)}{Dt} = v_t(x,t) + v(x,t)v_x(x,t),$$

where

$$v(x,t) = V(\rho(x,t), w(x,t)), \quad v_t = V_\rho \rho_t + V_w w_t, \quad v_x = V_\rho \rho_x + V_w w_x.$$

By simple computations, for the GSOM we have

$$a(x,t) = V_\rho\,(\rho_t + v\rho_x) = -V_\rho \rho v_x. \tag{5.6}$$

Once $\rho^n_{r,j}$, $w^n_{r,j}$ and $V^n_{r,j}$ are known, from Eq (5.6) we get the discrete acceleration

$$a^n_{r,j} = -V_\rho(\rho^n_j, w^n_j)\rho^n_j \frac{v^n_{j+1} - v^n_{j-1}}{2\Delta x}.$$

Then, we compute the emission rate by adapting equation (4.1) to the numerical framework. Hence, for each time t^n and cell x_j, $j = 1, \dots, N_x$, of road r we define

$$E^n_{r,j} = \rho^n_{r,j}\Delta x_j \max\{E_0, f_1 + f_2 v^n_{r,j} + f_3 (v^n_{r,j})^2 + f_4 a^n_{r,j} + f_5 (a^n_{r,j})^2 + f_6 v^n_{r,j} a^n_{r,j}\}, \tag{5.7}$$

where $E_0 = 0$ and the coefficients f_1 to f_6 are collected in Table 1.

The functional $\mathcal{F}(\gamma)$ in Eq (4.3) is then discretized as

$$\mathcal{F}(\gamma) \approx \frac{1}{N_x N_t N_r} \sum_{r=1}^{N_r} \sum_{n=1}^{N_t} \sum_{j=1}^{N_x} \left[\frac{E^\gamma_r(x_j, t^n)}{E^{\max}} + \frac{\varepsilon}{\mathcal{V}^\gamma_r(x_j, t^n)} \right], \tag{5.8}$$

where $E^{\max}$ is the maximum emission rate, ε is the rounded minimum velocity, and, in order to have comparable quantities for the emission and travel time functional, the weights c_1 and c_2 are given by

$$c_1 = \frac{1}{E^{\max} N_x N_t N_r} \qquad \text{and} \qquad c_2 = \frac{\varepsilon}{N_x N_t N_r}. \tag{5.9}$$

From now on we assume $\varepsilon = 1\,\text{km/h}$. As shown in Appendix A, this choice of weights does not substantially affect the numerical results described in the following sections. Thus $\mathcal{F}$ in Eqs (5.8) and (5.9) is an appropriate functional to analyze the cost in emission and travel time.

6. Case study of a merge junction

Let us consider the merge junction depicted in Figure 3, where we assume road 1 to be a ramp merging to roads 2 and 3. We assume the junction to be governed first by a priority rule and then by a traffic light. The latter is modeled by alternating $\beta = 0$ and $\beta = 1$ in time.

The model parameters in Eq (5.1) and those for the numerical tests are fixed in Table 2. The initial data is assumed to be constant on all the three roads and is chosen according to Table 3.

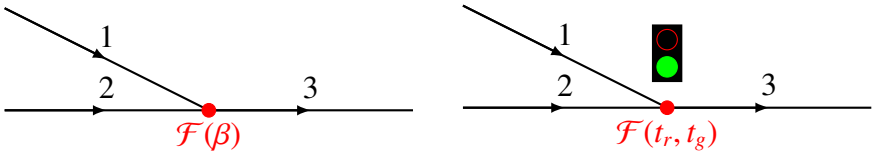

(a) priority rule **(b)** traffic light

Figure 3. Example of merge junction where road 1 joins roads 2 and 3.

Table 2. Parameters used for the numerical tests.

ρ_f	$\rho^{\max}$	ρ_c	$V^{\max}$	L	Δx	T	Δt
19 veh/km	133 veh/km	67.5 veh/km	70 km/h	3 km	100 m	10 min	4 s

Table 3. Initial data for the test on a merge junction, with $w_M = (w_R + w_L)/2$. We assume fast drivers coming from road 1 and moderate drivers on road 2 and 3.

Road r	1	2	3
ρ_r^0 (veh/km)	12	60	60
w_r^0	w_R	w_M	w_M

First we focus on the emission functional

$$\mathcal{F}_E(\gamma) \approx \frac{1}{N_x N_t N_r E^{\max}} \sum_{r=1}^{N_r} \sum_{n=1}^{N_t} \sum_{j=1}^{N_x} E_r^{\gamma}(x_j, t^n).$$

We look for the parameter $\beta \in [0, 1]$ which minimizes $\mathcal{F}_E(\beta)$, and analyze the RP algorithm given in Definition 3.1. In Figure 4 on the left, we show $\mathcal{F}_E(\beta)$ for β varying in $[0, 1]$. The optimal priority rule is given by $\beta^{opt} = 0$, i.e., no vehicle enters the junction from road 2. This result is unrealistic and thus motivates the use of the extended functional (4.3) including travel times. In Figure 4 on the right, we then show the test result for functional $\mathcal{F}$ with $\varepsilon = 1$ km/h. The optimal parameter is $\beta^{opt} = 0.64$ and $\mathcal{F}(\beta^{opt}) = 8.10$ which is an admissible and realist solution.

Optimal traffic light We model a traffic light placed at the end of roads 1 and 2 (see Figure 3b) by alternating $\beta = 0$ and $\beta = 1$ in time. Specifically, for $\beta = 0$ the traffic light is green for road 1 and red for road 2, on the contrary for $\beta = 1$ it is red for road 1 and green for road 2. The controls are given by the green phase duration t_g (when $\beta = 0$) and red phase duration t_r (when $\beta = 1$). The problem (4.4) is studied for $\Gamma = G \times R \subset \mathbb{R}^2$, where G and R are the intervals where t_g and t_r vary, and the cost functional $\mathcal{F}(\gamma) = \mathcal{F}(t_g, t_r)$. Fixing $G = R = [0, 90\,\text{s}]$, in Figure 5 we plot $\mathcal{F}(t_g, t_r)$ with initial traffic data given in Table 3. The optimal times are $t_g^{opt} = 5$ s and $t_r^{opt} = 10$ s and $\mathcal{F}(t_g^{opt}, t_r^{opt}) = 8.18$. We observe that the region bounded by dark-blue lines identifies the points with functional values close to the minimum one. Therefore, many couples (t_g, t_r) allow to have low emissions and travel time.

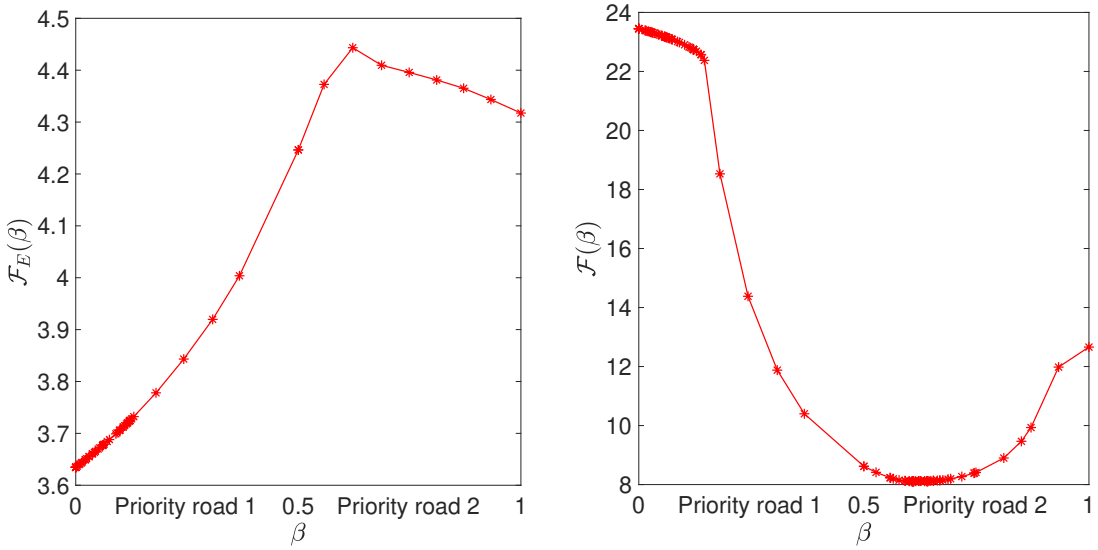

(a) $\mathcal{F}_E(\beta)$ with RP algorithm.

(b) $\mathcal{F}(\beta)$ with RP algorithm.

Figure 4. Case study of a merge junction. $\mathcal{F}_E(\beta)$ (left) and $\mathcal{F}(\beta)$ (right) as β changes in $[0, 1]$ using the RP algorithm. The initial data is given in Table 3.

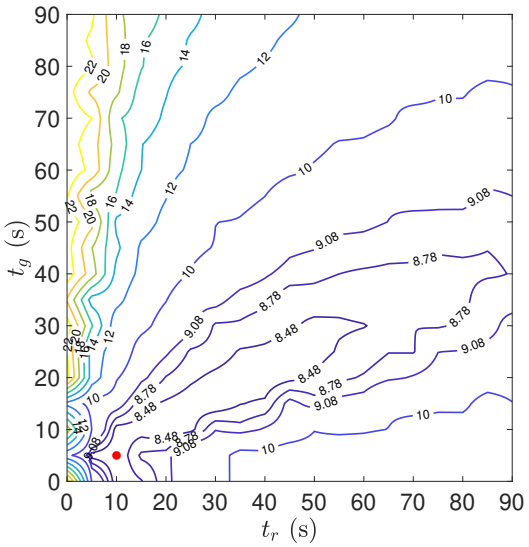

Figure 5. $\mathcal{F}(t_g, t_r)$ as t_g and t_r vary in $[0, 90\,\text{s}]$ with initial data in Table 3. In red the optimal point $(t_g^{opt}, t_r^{opt}) = (5\,\text{s}, 10\,\text{s})$.

In summary, in Table 4 we compare the minimum values of $\mathcal{F}_E(\gamma)$, $\mathcal{F}_T(\gamma)$ and $\mathcal{F}(\gamma)$ obtained with $\gamma = \beta^{opt}$ and $\gamma = (t_g^{opt}, t_r^{opt})$. The optimal values are very close. The numerical tests show that $\mathcal{F}$ has a convex shape, both with respect to β^{opt} and (t_g^{opt}, t_r^{opt}).

6.1. Sensitivity to initial data

Here we investigate numerically the sensitivity of the minimization problem (4.4) with respect to the initial traffic states for constant initial data on all three roads. We consider two different traffic

Table 4. Comparison of $\mathcal{F}_E(\gamma)$, $\mathcal{F}_T(\gamma)$ and $\mathcal{F}(\gamma)$ for $\gamma = \beta^{opt}$ and $\gamma = (t_g^{opt}, t_r^{opt})$.

Optimal Control	Value	$\mathcal{F}_E$	$\mathcal{F}_T$	$\mathcal{F}$
β^{opt}	0.64	4.45	3.66	8.05
t_g^{opt}, t_r^{opt}	5 s, 10 s	4.39	3.78	8.18

scenarios:

(i) $\rho_{2,3}^0 < \rho_f$, i.e. *free flow* traffic conditions on roads 2 and 3. Specifically, we fix $\rho_2^0 = \rho_3^0 = 15$ veh/km and $w_2^0 = w_3^0 = (w_L + w_R)/2$ along the roads;

(ii) $\rho_{2,3}^0 > \rho_f$, i.e. *congested* traffic conditions on roads 2 and 3. Specifically, we fix $\rho_2^0 = \rho_3^0 = 60$ veh/km and $w_2^0 = w_3^0 = (w_L + w_R)/2$ along the roads.

The optimal control is computed as function of the initial datum on road 1: $(\rho_1^0, w_1^0) \in [0, \rho^{\max}] \times [w_L, w_R]$.

Priority rule We focus on RP algorithm. Recall that values of $\beta < 0.5$ give the priority to road 1, while values of $\beta > 0.5$ give the priority to road 2. In Figure 6 we highlight the level curve related to $\beta = 0.5$ using a bold line. In Figure 6a we show the result for the *free-flow* case (i). The optimal priority β^{opt} decreases as ρ_1^0 increases. Specifically, if $\rho_1^0 < \rho_2^0 = \rho_3^0 = 15$ veh/km then road 2 should have the priority and β^{opt} is independent of the speed attitude of drivers w_1^0. On the other hand, if $\rho_1^0 > 15$ veh/km then road 1 should have the priority. In this case, β^{opt} depends on w_1^0. In fact, it decreases more rapidly for high values of w_1^0. Hence, vehicles with fast drivers should cross the junction in a higher percentage $(1 - \beta)$ than vehicles with slow drivers. In Figure 6b we show the result for the *congested* case (ii). As before β^{opt} decreases as ρ_1^0 increases. We observe that road 2 should always have the priority when slow drivers ($w_1^0 = w_L$) arrive from road 1. On the other hand, road 1 should have the priority for high values of ρ_1^0 and w_1^0 (region to the right of the curve $\beta^{opt} = 0.5$).

Traffic light Here we analyze how the ratio between the optimal green and red duration t_g^{opt}/t_r^{opt} varies with respect to (ρ_1^0, w_1^0) for the two traffic scenarios (i) and (ii). In Figure 7 we show the result for the *free-flow* case (i). The left plot represents the level curves of $\mathcal{F}$ computed with the optimal couple (t_g^{opt}, t_r^{opt}): the minimum value is increasing in ρ_1^0 independently of w_1^0; the dependence on w_1^0 only occurs when many slow vehicles arrive from road 1 (bottom right of the figure). The right plot shows the level curves of the ratio t_g^{opt}/t_r^{opt}, where the bold line identifies the curve with $t_g^{opt}/t_r^{opt} = 1$. We observe that for small values of ρ_1^0, the red phase should be longer than the green one. On the other hand, when ρ_1^0 increases, the ratio becomes greater than one, and thus vehicles coming from road 1 should have a longer green phase. Again, the solution is not very sensitive to the variations of the speed attitude of drivers w_1^0. In Figure 8 we show the result for the *congested* case (ii). The behavior of $\mathcal{F}(t_g^{opt}, t_r^{opt})$ on the left plot is analogous to case (i), while the trend of the ratio t_g^{opt}/t_r^{opt} changes. Indeed, the green phase should be longer than the red one only for high values of ρ_1^0 and low values of w_1^0. Finally we observe that in both cases, the minimum of the functional is not very sensitive to small perturbations of optimal (t_g^{opt}, t_r^{opt}).

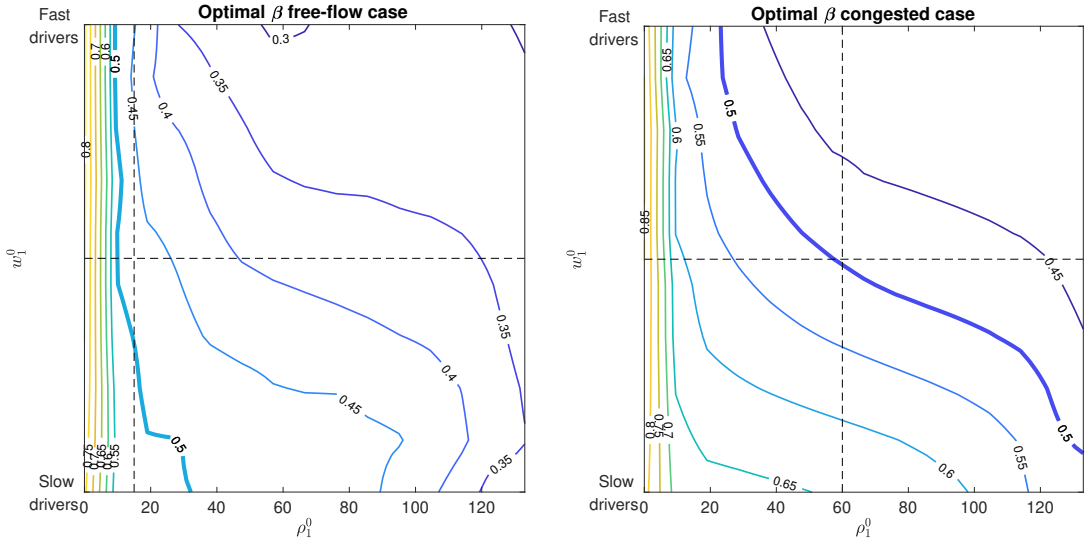

(a) Free-flow case: $\rho_0^2 = \rho_0^3 = 15$ veh/km, $w_0^2 = w_0^3 = (w_L + w_R)/2$ (dashed lines).

(b) Congested case: $\rho_0^2 = \rho_0^3 = 60$ veh/km, $w_0^2 = w_0^3 = (w_L + w_R)/2$ (dashed lines).

Figure 6. Sensitivity to initial data: optimal priority rule as ρ_0^1 and w_0^1 change. In (a) the free-flow case (i); In (b) the congested case (ii). When $\beta < 0.5$ road 1 has the priority, otherwise road 2 has the priority.

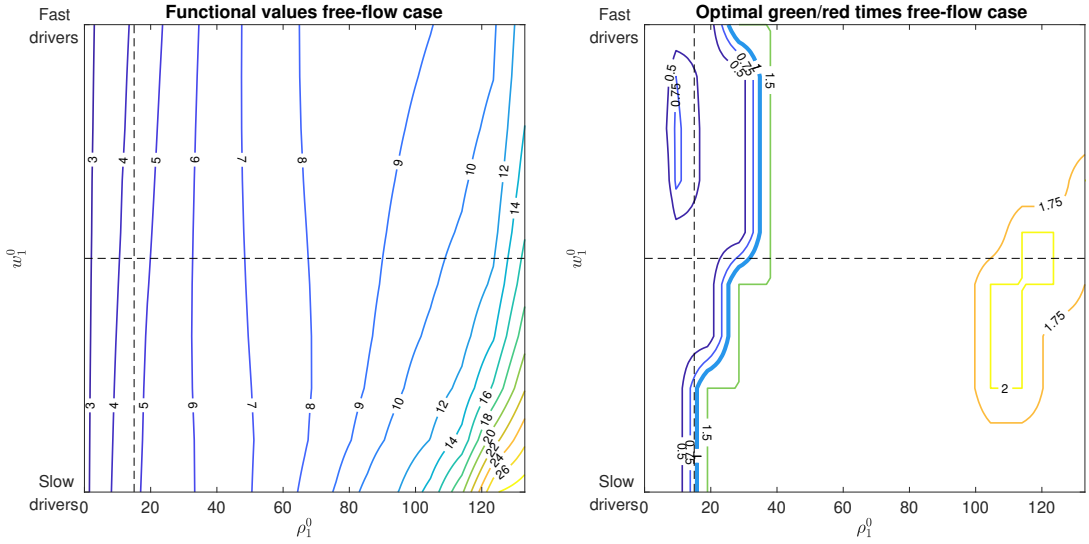

(a) Level curves of $\mathcal{F}$ computed with (t_g^{opt}, t_r^{opt}).

(b) Level curves of t_g^{opt}/t_r^{opt} ratio.

Figure 7. Sensitivity to initial data: optimal traffic light timing as ρ_1^0 and w_1^0 change. Roads 2 and 3 start in the free-flow phase: $\rho_2^0 = \rho_3^0 = 15$ veh/km and $w_2^0 = w_3^0 = (w_L + w_R)/2$ (dashed lines).

We can summarize the results as follows. For the priority-ruled junction, we obtain the minimum of the functional $\mathcal{F}$ by giving the priority to the incoming road with higher density and favoring fast drivers. For the traffic light too, the road with higher density should have a longer green phase. However, when the three roads are congested, vehicles with slow drivers should have a longer green phase. As

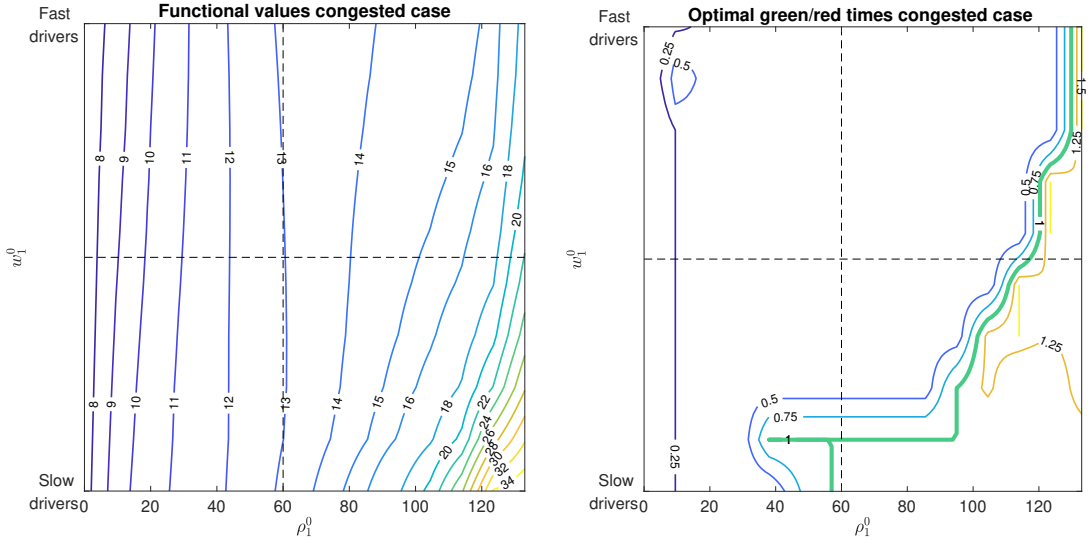

(a) Level curves of $\mathcal{F}$ computed with (t_g^{opt}, t_r^{opt}).

(b) Level curves of t_g^{opt}/t_r^{opt} rate.

Figure 8. Sensitivity to initial data: optimal traffic light timing as ρ_1^0 and w_1^0 change. Roads 2 and 3 start in the congested phase: $\rho_2^0 = \rho_3^0 = 60$ veh/km and $w_2^0 = w_3^0 = (w_L + w_R)/2$ (dashed lines).

expected, the sensitivity with respect to w is greater when traffic is congested, that is when it is more influenced by w.

7. Emissions at roundabouts

In this section we study emissions and travel times for a roundabout, modeled combining merge and diverge junctions as depicted in Figure 9. There are four junctions: J_1 and J_3 of type $2 \to 1$ (merge); J_2 and J_4 of type $1 \to 2$ (diverge). We focus on the AP algorithm to compute the minimum of problem (4.4), obtaining the priority parameters $\gamma = (\beta_{J_1}, \beta_{J_3}) \in [0,1]^2$. We also compute the optimal timing $\gamma = ((t_g, t_r)_{J_1}, (t_g, t_r)_{J_3}) \in [G \times R]^2$ for the roundabout with traffic lights placed at the two merge junctions J_1 and J_3, with $G = R = [25\,\text{s}, 90\,\text{s}]$. We exclude traffic light phases smaller than 25 s, and compare the roundabout with priorities with that with traffic lights. Furthermore, we consider the case of periodic traffic lights with $(t_g, t_r)_{J_1} = (t_g, t_r)_{J_3} = (45\,\text{s}, 45\,\text{s})$ to compare the optimal traffic lights with naive ones.

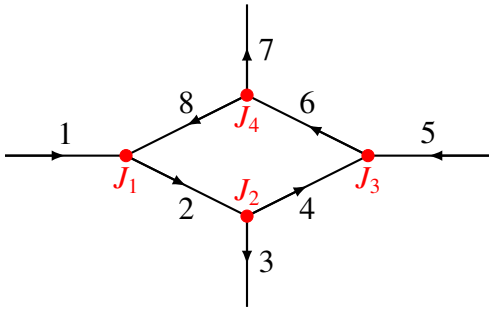

Figure 9. Example of roundabout.

The two diverging junctions J_2 and J_4 have a fixed distribution parameter $\alpha = 0.6$. The model parameters ρ_f, $\rho^{\max}$, ρ_c and $V^{\max}$, the length of the roads L and the space step Δx are fixed as in Table 2. The length of the simulations is $T = 1\,\text{h}$ and the time step $\Delta t = 2.57\,\text{s}$. The initial density is assumed to be null for each road. We analyze three traffic scenarios determined by the density of vehicles which enter into the network from roads 1 and 5. On the latter, we used Dirichlet boundary conditions:

$$\rho^n_{r,0} = \begin{cases} \bar{\rho} & \text{if } t^n \leq 20 \text{ min} \\ 0 & \text{otherwise} \end{cases} \qquad \bar{\rho} = 15, 40 \text{ or } 80 \text{ veh/km} \tag{7.1}$$

and $w^n_{0,r} = (w_L + w_R)/2$ for $r = 1, 5$. We use Neumann boundary conditions for roads 3 and 7, thus allowing all vehicles to exit the roundabout. The initially empty network is filled up for the first 20 min of simulation, then no more vehicles access the network until the final time $T = 1\,\text{h}$. In this way, the emissions are measures both for loading and unloading of the roundabout.

Table 5. Comparison of $\mathcal{F}_E(\gamma)$, $\mathcal{F}_T(\gamma)$ and $\mathcal{F}(\gamma)$ for γ chosen as the optimal controls on the junctions J_1 and J_3 of the network for different Dirichlet boundary conditions.

$\bar{\rho}$ (veh/km)	Control		Value	$\mathcal{F}_E$	$\mathcal{F}_T$	$\mathcal{F}$
15	Optimal	β_{J_1}, β_{J_3}	0.50, 0.50	0.46	1.52	1.98
	Optimal	$(t_g, t_r)_{J_1}$ $(t_g, t_r)_{J_3}$	62 s, 26 s 27 s, 47 s	0.36	1.49	1.86
	Periodic	$(t_g, t_r)_{J_1}$ $(t_g, t_r)_{J_3}$	45 s, 45 s 45 s, 45 s	0.39	1.76	2.15
40	Optimal	β_{J_1}, β_{J_3}	0.34, 0.69	1.04	1.81	2.85
	Optimal	$(t_g, t_r)_{J_1}$ $(t_g, t_r)_{J_3}$	69 s, 29 s 27 s, 44 s	0.92	1.91	2.84
	Periodic	$(t_g, t_r)_{J_1}$ $(t_g, t_r)_{J_3}$	45 s, 45 s 45 s, 45 s	0.98	2.62	3.60
80	Optimal	β_{J_1}, β_{J_3}	0.34, 0.68	1.15	1.88	3.02
	Optimal	$(t_g, t_r)_{J_1}$ $(t_g, t_r)_{J_3}$	69 s, 29 s 27 s, 44 s	1.03	1.99	3.02
	Periodic	$(t_g, t_r)_{J_1}$ $(t_g, t_r)_{J_3}$	45 s, 45 s 45 s, 45 s	1.08	2.77	3.85

In Table 5 we show the optimal controls and the corresponding functionals values. We observe that $\mathcal{F}_E$, $\mathcal{F}_T$ and $\mathcal{F}$ grow as the number of vehicles entering the network increases, both for priorities and traffic lights dynamics. In particular, in the case of $\bar{\rho} = 15\,\text{veh/km}$ in Eq (7.1), the traffic lights dynamics produce 20% lower emissions and 2% lower travel times with respect to priorities. In congested situations, instead, the emissions are reduced by about 11% in presence of traffic lights, while the travel times are 6% longer compared to priority-ruled dynamics. Moreover, for all the boundary data $\bar{\rho}$ the dynamics with periodic traffic lights produce higher emissions and longer travel

times compared to the dynamics with optimized traffic lights; in congested situations the increase of $\mathcal{F}$ is about 30%. On the other hand, periodic traffic lights produce lower emissions than optimized priorities dynamics, but significantly higher travel times. The higher levels of emissions associated with priorities can be observed also in Figure 10, where we plot the emissions on each road of the network at different times. The emissions associated with traffic lights dynamics show an oscillating behavior which is not observed in the priorities case, see plots in Figures 10a–e. At the final time of the simulation, plots Figures 10c and 10f, the emissions are close to 0 as nearly all vehicles have left the network.

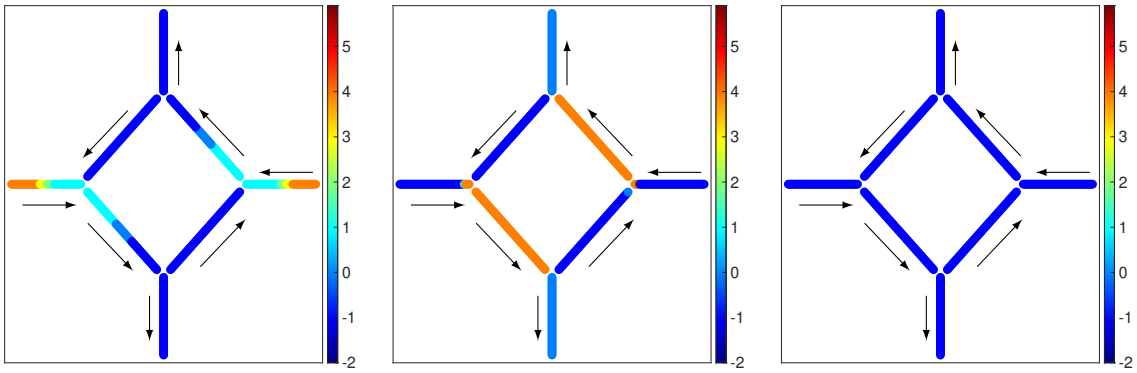

(a) Optimal priority: NO_x at t = 5 min.

(b) Optimal priority: NO_x at t = 30 min.

(c) Optimal priority: NO_x at t = 1 h.

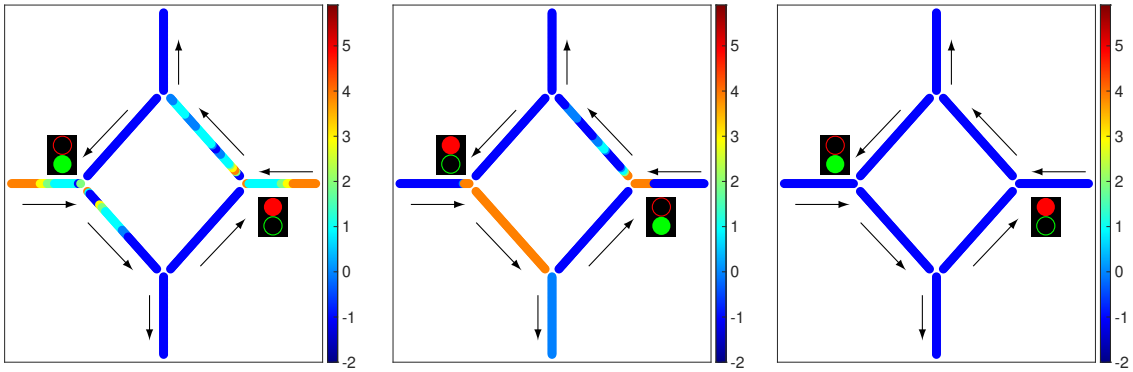

(d) Optimal traffic light: NO_x at t = 5 min.

(e) Optimal traffic light: NO_x at t = 30 min.

(f) Optimal traffic light: NO_x at t = 1 h.

Figure 10. NO_x emission rates (g/h) on a network with priority rules (top) and traffic lights (bottom) in J_1 and J_3.

Finally, in Figure 11, we show the change in time of the total emission rates in the whole network. The trend in emission rates is the same for the three cases: emissions rise as vehicles enter the network and then decrease to 0. The peak value grows as $\bar{\rho}$ increases. Again, periodic traffic lights correspond to higher emissions than optimized ones. In Table 6 we report the total number of vehicles that enter the network for the three tests and the corresponding total amount of emissions produced with the two optimized traffic dynamics. We observe that emissions are more than double when $\bar{\rho} = 40$ veh/km compared to $\bar{\rho} = 15$ veh/km and almost triple when $\bar{\rho} = 80$ veh/km with respect to $\bar{\rho} = 15$ veh/km, while the difference between the case of $\bar{\rho} = 40$ veh/km and the one of $\bar{\rho} = 80$ veh/km is smaller.

To check the robustness of our results, we computed the minima of the functional $\mathcal{F}$ for different values of the weights c_1 and c_2 in Appendix A. The specific values of the functional obviously varies as we change the weights, but not the qualitative and quantitative comparison of priorities with traffic lights. Moreover, the optimal traffic light timing appears to be more robust than the optimal priorities.

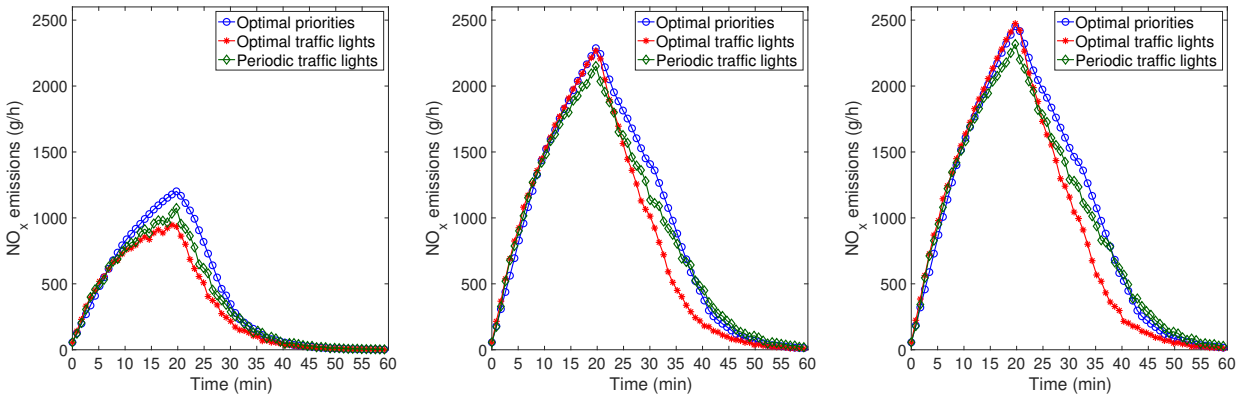

(a) $\bar{\rho} = 15$ veh/km **(b)** $\bar{\rho} = 40$ veh/km **(c)** $\bar{\rho} = 80$ veh/km

Figure 11. Total NO_x emission rates (g/h) along the whole roundabout.

Table 6. Total number of vehicles entering the network and total amount of emissions produced for the three cases analyzed.

$\bar{\rho}$ (veh/km)	Total vehicles	Total emissions priorities (g/h)	Total emissions traffic lights (g/h)
15	620	576328	458563
40	961	1316544	1169322
80	1012	1450627	1299261

8. Conclusions

In this work, we have extended the Generic Second Order Model to a road network with merge and diverge junctions and proposed a tool to estimate and minimize traffic emissions by regulating traffic dynamics. Such regulation corresponds to the choice of suitable model parameter γ that governs the distribution of traffic in a diverge and priorities in a merge.

Different scenarios have been considered, such as: a traffic policeman who strictly enforces the priority rule (RP algorithm), an uncontrolled intersection where drivers tend to maximize the flow (AP algorithm), and the presence of a traffic light. A functional measuring emissions and travel times was tested numerically on a single merge junction, showing that the minimum is achieved by giving the priority and a longer green traffic light to the incoming road with higher density and fast drivers. On the other hand, the test performed on a roundabout has pointed out that traffic lights appear to be convenient with respect to priorities for emissions, especially at low densities. This indicates that the increasingly common roundabouts may benefit from the installation of traffic lights at entrances. We

conclude by stating that our approach is very flexible and can easily be used as a decision support for traffic management.

Acknowledgments

C. B. and M. B. acknowledge the Italian Ministry of University and Research (MUR) for supporting this research with funds coming from the PRIN Project 2017 "Innovative numerical methods for evolutionary partial differential equations and applications" (No. 2017KKJP4X). This work was carried out within the research project "SMARTOUR: Intelligent Platform for Tourism" (No. SCN 00166) funded by the MUR with the Regional Development Fund of European Union (PON Research and Competitiveness 2007–2013). C. B. and M. B. are members of the INdAM Research group GNCS. The research of B. P. was partially supported by the NSF CPS Synergy project "Smoothing Traffic via Energy-efficient Autonomous Driving" (STEAD) CNS 1837481. The research of B. P. is based upon work supported by the U.S. Department of Energy's Office of Energy Efficiency and Renewable Energy (EERE) under the Vehicle Technologies Office award number CID DE-EE0008872. The views expressed herein do not necessarily represent the views of the U.S. Department of Energy or the United States Government.

Conflict of interest

The authors declare that there is no conflict of interest.

References

1. L. J. Alvarez-Vázquez, N. García-Chan, A. Martínez, M. E. Vázquez-Méndez, Numerical simulation of air pollution due to traffic flow in urban networks, *J. Comput. Appl. Math.*, **326** (2017), 44–61. https://doi.org/10.1016/j.cam.2017.05.017
2. L. J. Alvarez-Vázquez, N. García-Chan, A. Martínez, M. E. Vázquez-Méndez, Optimal control of urban air pollution related to traffic flow in road networks, *Math. Control Relat. F.*, **8** (2018), 177–193. https://doi.org/10.3934/mcrf.2018008
3. C. Appert-Rolland, F. Chevoir, P. Gondret, S. Lassarre, J. P. Lebacque, M. Schreckenberg, *Traffic and granular flow '07*, Berlin: Springer-Verlag, 2009.
4. R. Atkinson, W. P. Carter, Kinetics and mechanisms of the gas-phase reactions of ozone with organic compounds under atmospheric conditions, *Chem. Rev.*, **84** (1984), 437–470. https://doi.org/10.1021/cr00063a002
5. A. Aw, M. Rascle, Resurrection of "Second Order" Models of Traffic Flow, *SIAM J. Appl. Math.*, **60** (2000), 916–944. https://doi.org/10.1137/S0036139997332099
6. C. Balzotti, Second order traffic flow models on road networks and real data applications, Doctoral Thesis of Sapienza University, Rome, 2021.
7. C. Balzotti, M. Briani, B. De Filippo, B. Piccoli, A computational modular approach to evaluate NO_x emissions and ozone production due to vehicular traffic, *Discrete Cont. Dyn.-B*, **27** (2022), 3455–3486.

8. S. Blandin, D. Work, P. Goatin, B. Piccoli, A. Bayen, A General Phase Transition Model for Vehicular Traffic, *SIAM J. Appl. Math.*, **71** (2011), 107–127. https://doi.org/10.1137/090754467
9. G. M. Coclite, M. Garavello, B. Piccoli, Traffic flow on a road network, *SIAM J. Math. Anal.*, **36** (2005), 1862–1886. https://doi.org/10.1137/S0036141004402683
10. R. M. Colombo, Hyperbolic Phase Transitions in Traffic Flow, *SIAM J. Appl. Math.*, **63** (2003), 708–721. https://doi.org/10.1137/S0036139901393184
11. R. M. Colombo, P. Goatin, B. Piccoli, Road networks with phase transitions, *J. Hyperbolic Differ. Equ.*, **7** (2010), 85–106. https://doi.org/10.1142/S0219891610002025
12. C. F. Daganzo, Requiem for second-order fluid approximations of traffic flow, *Transp. Res. B*, **29** (1995), 277–286. https://doi.org/10.1016/0191-2615(95)00007-Z
13. M. L. Delle Monache, P. Goatin, B. Piccoli, Priority-based Riemann solver for traffic flow on networks, *Commun. Math. Sci.*, **16** (2018), 185–211. https://doi.org/10.4310/CMS.2018.v16.n1.a9
14. S. Fan, M. Herty, B. Seibold, Comparative model accuracy of a data-fitted generalized Aw-Rascle-Zhang model, *Netw. Heterog. Media*, **9** (2014), 239–268. https://doi.org/10.3934/nhm.2014.9.239
15. S. Fan, B. Seibold, Data-fitted first-order traffic models and their second-order generalizations: Comparison by trajectory and sensor data, *Transp. Res. Rec.*, **2391** (2013), 32–43. https://doi.org/10.3141/2391-04
16. S. Fan, Y. Sun, B. Piccoli, B. Seibold, D. B. Work, *A Collapsed Generalized Aw-Rascle-Zhang Model and its Model Accuracy*, arXiv:1702.03624, [Preprint], (2017) [cited 2023 Feb 22]. Available from: https://doi.org/10.48550/arXiv.1702.03624
17. M. Garavello, K. Han, B. Piccoli, *Models for Vehicular Traffic on Networks*, Springfield: American Institute of Mathematical Sciences, 2016.
18. M. Garavello, B. Piccoli, *Traffic flow on networks*, Springfield: American Institute of Mathematical Sciences, 2006.
19. M. Garavello, B. Piccoli, Traffic flow on a road network using the Aw-Rascle Model, *Commun. Partial. Differ. Equ.*, **31** (2006), 243–275. https://doi.org/10.1080/03605300500358053
20. M. Garavello, B. Piccoli, Conservation laws on complex networks, *Ann. Inst. H. Poincaré Anal. Non Linéaire*, **26** (2009), 1925–1951. https://doi.org/10.1016/j.anihpc.2009.04.001
21. M. Garavello, B. Piccoli, Coupling of Lighthill-Whitham-Richards and phase transition models, *J. Hyperbolic Differ. Equ.*, **10** (2013), 577–636. https://doi.org/10.1142/S0219891613500215
22. N. García-Chan, L. J. Alvarez-Vázquez, A. Martínez, M. E. Vázquez-Méndez, Numerical simulation for evaluating the effect of traffic restrictions on urban air pollution, *Progress in Industrial Mathematics at ECMI 2016*, Springer International Publishing, 2017, 367–373.
23. M. Herty, S. Moutari, M. Rascle, Optimization criteria for modelling intersections of vehicular traffic flow, *Netw. Heterog. Media*, **1** (2006), 275–294. https://doi.org/10.3934/nhm.2006.1.275
24. M. Herty, M. Rascle, Coupling conditions for a class of second-order models for traffic flow, *SIAM J. Math. Anal.*, **38** (2006), 595–616. https://doi.org/10.1137/05062617X
25. H. Holden, N. H. Risebro, A mathematical model of traffic flow on a network of unidirectional roads, *SIAM J. Math. Anal.*, **26** (1995), 999–1017. https://doi.org/10.1137/S0036141093243289

26. Y. Huang, C. Lei, C. H. Liu, P. Perez, H. Forehead, S. Kong, J. L. Zhou, A review of strategies for mitigating roadside air pollution in urban street canyons, *Environ. Pollut.*, **280** (2021), 116971. https://doi.org/10.1016/j.envpol.2021.116971

27. A. Khelifi, H. Haj-Salem, J. P. Lebacque, L. Nabli, Lagrangian generic second order traffic flow models for node, *J. Traffic Transp. Eng.*, **5** (2018), 14–27. https://doi.org/10.1016/j.jtte.2017.08.001

28. O. Kolb, G. Costeseque, P. Goatin, S. Göttlich, Pareto-optimal coupling conditions for the Aw-Rascle-Zhang traffic flow model at junctions, *SIAM J. Appl. Math.*, **78** (2018), 1981–2002. https://doi.org/10.1137/17M1136900

29. J. P. Lebacque, S. Mammar, H. Haj-Salem, Generic second order traffic flow modelling, *Transportation and Traffic Theory*, Netherlands: Elsevier, 2007, 755–776.

30. J. P. Lebacque, A two phase extension of the LWR model based on the boundedness of traffic acceleration,*Transportation and Traffic Theory in the 21st Century*, Bradford: Emerald Group Publishing Limited, 2002.

31. M. J. Lighthill, G. B. Whitham, On kinematic waves II. A theory of traffic flow on long crowded roads, *Proc. Roy. Soc. A*, **229** (1955), 317–345. https://doi.org/10.1098/rspa.1955.0089

32. L. I. Panis, S. Broekx, R. Liu, Modelling instantaneous traffic emission and the influence of traffic speed limits, *Sci. Total Environ.*, **371** (2006), 270–285. https://doi.org/10.1016/j.scitotenv.2006.08.017

33. H. J. Payne, Models of freeway traffic and control, *Proc. Simulation Council*, **1** (1971), 51–61.

34. B. Piccoli, K. Han, T. L. Friesz, T. Yao, J. Tang, Second-order models and traffic data from mobile sensors, *Transport. Res. C-Emer.*, **52** (2015), 32–56. https://doi.org/10.1016/j.trc.2014.12.013

35. P. I. Richards, Shock Waves on the Highway, *Operations Research*, **4** (1956), 42–51. https://doi.org/10.1287/opre.4.1.42

36. S. Samaranayake, S. Glaser, D. Holstius, J. Monteil, K. Tracton, E. Seto, A. Bayen, Real-time estimation of pollution emissions and dispersion from highway traffic, *Comput-Aided Civ. Inf.*, **29** (2014), 546–558.

37. S. Vardoulakis, B. E. Fisher, K. Pericleous, N. Gonzalez-Flesca, Modelling air quality in street canyons: a review, *Atmos. Environ.*, **37** (2003), 155–182. https://doi.org/10.1016/S1352-2310(02)00857-9

38. G. B. Whitham, *Linear and nonlinear waves*, New York: John Wiley and Sons,1974.

39. H. M. Zhang, A non-equilibrium traffic model devoid of gas-like behavior, *Transp. Res. B*, **36** (2002), 275–290. https://doi.org/10.1016/S0191-2615(00)00050-3

40. K. Zhang, S. Batterman, Air pollution and health risks due to vehicle traffic, *Sci. Total Environ.*, **450** (2013), 307–316. https://doi.org/10.1016/j.scitotenv.2013.01.074

A. Senstivity of $\mathcal{F}$ to weights c_1 and c_2

In this appendix we investigate the sensitivity of the functional $\mathcal{F}$ with respect to the weights c_1 and c_2 in Eq (5.9) for the roundabout. Our aim is to compare the optimal controls obtained by giving more

importance once to emissions and once to the travel time. Therefore, we define $\mathcal{F}_{c_1} = \kappa c_1 \mathcal{F}_E + c_2 \mathcal{F}_T$ and $\mathcal{F}_{c_2} = c_1 \mathcal{F}_E + \kappa c_2 \mathcal{F}_T$ with $\kappa = 10, 100$.

In Tables A1 and A2 we report the optimal controls computed for $\mathcal{F}_{c_1}$ and $\mathcal{F}_{c_2}$, using the Dirichlet boundary conditions in Eq (7.1) for different $\bar{\rho}$ as in Section 7. First, we observe that the values of the functional $\mathcal{F}_{c_1}$ are lower than those of the functional $\mathcal{F}_{c_2}$. Therefore, giving more importance to emissions rather than to travel time allows to reduce the total cost. Analogously to the case of functional $\mathcal{F}$ studied in Section 7, in all cases traffic lights dynamics are convenient in terms of emissions production, while the travel time is shorter when traffic is ruled by priorities. Finally, note that the optimal priorities are influenced by the choice of the functional, while the optimal traffic light timing is always the same for all the tests.

Table A1. Comparison of $\mathcal{F}_E(\gamma)$, $\mathcal{F}_T(\gamma)$, $\mathcal{F}_{c_1}(\gamma)$ and $\mathcal{F}_{c_2}(\gamma)$ for γ chosen as the optimal controls on junctions J_1 and J_3 for different boundary $\bar{\rho}$ (veh/km) and $\kappa = 10$.

(a) $\mathcal{F}_{c_1} = 10\mathcal{F}_E + \mathcal{F}_T$

$\bar{\rho}$	Optimal control	Value	$\mathcal{F}_E$	$\mathcal{F}_T$	$\mathcal{F}_{c_1}$
15	β_{J_1}, β_{J_3}	0.50, 0.50	0.46	1.52	6.08
	$(t_g, t_r)_{J_1}$ $(t_g, t_r)_{J_3}$	62 s, 26 s 27 s, 47 s	0.36	1.49	5.12
40	β_{J_1}, β_{J_3}	0.28, 0.77	0.10	1.83	12.13
	$(t_g, t_r)_{J_1}$ $(t_g, t_r)_{J_3}$	69 s, 29 s 27 s, 44 s	0.92	1.91	11.16
80	β_{J_1}, β_{J_3}	0.45, 0.74	1.14	1.88	13.30
	$(t_g, t_r)_{J_1}$ $(t_g, t_r)_{J_3}$	69 s, 29 s 27 s, 44 s	1.03	1.99	12.26

(b) $\mathcal{F}_{c_2} = \mathcal{F}_E + 10\mathcal{F}_T$

$\bar{\rho}$	Optimal control	Value	$\mathcal{F}_E$	$\mathcal{F}_T$	$\mathcal{F}_{c_2}$
15	β_{J_1}, β_{J_3}	0.50, 0.50	0.46	1.52	15.68
	$(t_g, t_r)_{J_1}$ $(t_g, t_r)_{J_3}$	62 s, 26 s 27 s, 47 s	0.36	1.49	15.29
40	β_{J_1}, β_{J_3}	0.33, 0.67	1.04	1.81	19.17
	$(t_g, t_r)_{J_1}$ $(t_g, t_r)_{J_3}$	69 s, 29 s 27 s, 44 s	0.92	1.91	20.06
80	β_{J_1}, β_{J_3}	0.34, 0.14	1.15	1.88	19.94
	$(t_g, t_r)_{J_1}$ $(t_g, t_r)_{J_3}$	69 s, 29 s 27 s, 44 s	1.03	1.99	20.94

Table A2. Comparison of $\mathcal{F}_E(\gamma)$, $\mathcal{F}_T(\gamma)$, $\mathcal{F}_{c_1}(\gamma)$ and $\mathcal{F}_{c_2}(\gamma)$ for γ chosen as the optimal controls on junctions J_1 and J_3 for different boundary $\bar{\rho}$ (veh/km) and $\kappa = 100$.

(a) $\mathcal{F}_{c_1} = 100\mathcal{F}_E + \mathcal{F}_T$

$\bar{\rho}$	Optimal control	Value	$\mathcal{F}_E$	$\mathcal{F}_T$	$\mathcal{F}_{c_1}$
15	β_{J_1}, β_{J_3}	0.50, 0.50	0.45	1.52	47.08
	$(t_g, t_r)_{J_1}$ $(t_g, t_r)_{J_3}$	62 s, 26 s 27 s, 47 s	0.36	1.49	37.74
40	β_{J_1}, β_{J_3}	0.26, 0.98	1.01	2.06	103.53
	$(t_g, t_r)_{J_1}$ $(t_g, t_r)_{J_3}$	69 s, 29 s 27 s, 44 s	0.92	1.91	94.34
80	β_{J_1}, β_{J_3}	0.27, 0.98	1.12	2.17	114.10
	$(t_g, t_r)_{J_1}$ $(t_g, t_r)_{J_3}$	69 s, 29 s 27 s, 44 s	1.03	1.99	104.69

(b) $\mathcal{F}_{c_2} = \mathcal{F}_E + 100\mathcal{F}_T$

$\bar{\rho}$	Optimal control	Value	$\mathcal{F}_E$	$\mathcal{F}_T$	$\mathcal{F}_{c_2}$
15	β_{J_1}, β_{J_3}	0.50, 0.50	0.46	1.52	152.67
	$(t_g, t_r)_{J_1}$ $(t_g, t_r)_{J_3}$	62 s, 26 s 27 s, 47 s	0.36	1.49	149.68
40	β_{J_1}, β_{J_3}	0.33, 0.67	1.04	1.81	182.35
	$(t_g, t_r)_{J_1}$ $(t_g, t_r)_{J_3}$	69 s, 29 s 27 s, 44 s	0.92	1.91	192.32
80	β_{J_1}, β_{J_3}	0.33, 0.56	1.15	1.88	188.93
	$(t_g, t_r)_{J_1}$ $(t_g, t_r)_{J_3}$	69 s, 29 s 27 s, 44 s	1.03	1.99	200.13

AIMS Press